TH-PM-A1 EFFECTS OF TONICITY ON THE FORCE-VELOCITY RELATIONSHIP IN SINGLE STRIATED MUSCLE FIBERS. K.A.P. Edman and J.C. Hwang, Department of Pharmacology, University of Lund, S-223 62 Lund, Sweden.

Single semitendinosus muscle fibers of R. temporaria were mounted (0.5-1.2 °C) between a tension transducer and a lever that was operated by an electromagnetic puller. The position of the lever was monitored by a capacitance type transducer. A servo system operating the puller permitted recording of active tension at a fixed fiber length or shortening velocity at any predetermined load. The fiber was tetanized isometrically at 2-min intervals. Constant velocities were recorded after the fiber was released to shorten isotonically between 2.20 and 1.95 μm sarcomere lengths (monitored by laser diffraction). Recordings were made between 45 and 120 min after immersion of the fiber in one of the following solutions: 1. ordinary Ringer, 2. Ringer + 50 mM sucrose and 3. Ringer with NaCl reduced to 0.8 of normal. Force-velocity data were fitted with a hyperbola (least squares). The slightly reversed curvature at loads higher than 80 % of the measured isometric tension (P_o) (Mulieri, Mulieri and Edman, Fedn Proc. 1974. 33. 383) was evident in all solutions. Vmax in Ringer was 1.87± 0.22 (S.D., n=8) L./sec and decreased by 23.0± 6.2 % ($p<0.01$) in hypertonic Ringer and increased by 12.1± 4.2 % ($p<0.01$) in hypotonic Ringer. Similarly P_o (22.3± 2.9 N/cm^2 in ordinary Ringer) decreased by 12.5± 2.9 % ($p<0.001$) in hypertonic and increased by 8.9± 2.2 % ($p<0.001$) in hypotonic Ringer. A change in tonicity affects both the internal ionic strength and fiber width. Previous results suggest that Vmax and P_o are very little dependent on myofilament lattice width. The effects on Vmax and P_o described here may therefore by largely attributed to changes in ionic strength of the intracellular medium.

TH-PM-A2 THE EQUILIBRIUM NATURE OF THE FILAMENT LATTICE OF SKINNED MUSCLE FIBERS. Ernest W. April and Donald Wong* Dept. of Anatomy, College of P & S of Columbia Univ., New York City 10032.

It has been proposed (April, 1973, Biophys. Soc. Abs.) that the thick filament lattice in striated muscle may exist in more than one liquid-crystalline state: equilibrium and non-equilibrium. The equilibrium referred to within the myofilament lattice is that point of balance between long-range electrostatic repulsive forces and van der Waal's attractive forces and represents the point of minimum interaction energy; this state is exemplified by glycerinated muscle, skinned and extremely swollen fibers, all conditions in which the volume-limiting effect of the sarcolemma has been eliminated. In the non-equilibrium state, that of the living intact muscle fiber, the Donnan steady state across the sarcolemma determines the volume of the muscle fiber and hence the volume of the myofilament lattice so that attainment of a true equilibrium between van der Waal's forces and electrostatic forces is precluded. Evidence in support of this hypothesis can be drawn from X-ray diffraction studies which compare the lattice behavior of skinned and intact muscle fibers over a range of sarcomere length. In a plot of the reciprocal of the square of the interfilament spacing vs. sarcomere length, the regression line for the intact fiber passes through the origin, while the skinned fiber fails this test for constant volume. Hence, when the filament spacing of the skinned fiber is plotted against the sarcomere length, the data approximate a regression line in contrast to the isovolumic curve of the intact fiber. (Supported by USPHS, AM 15876).

TH-PM-A3 EFFECT OF [Ca^{++}] ON ATPASE AND FORCE GENERATION IN CHEMICALLY SKINNED MUSCLE FIBERS.

R.M. Levy*, Y. Umazume* and M.J. Kushmerick, Department of Physiology, Harvard Medical School, Boston, Mass. 02115.

One to three mm segments of briefly glycerinated single fiber preparations of frog semitendinosus were studied at sarcomere length ≈2.5μ at 21°-23°C. Only fibers which remained homogeneous when observed with a dissecting microscope were used. Both tension development and total ADP production in the same fiber were measured in contracting solutions at pCa = 6.8 ($0.3P_o$), pCa = 6.4 ($0.8P_o$) and pCa = 5.9 (P_o). Total ADP production was normalized to fiber length and tension-time integral because latency before contraction and isometric tension are [Ca^{++}] dependent. The following ratios were observed in 1-3 min. contractions:

		pmoles ADP	±S.D.	N
		mg tension·min·mm fiber		
pCa 6.8	11.5 ± 3.1			8
pCa 6.4	22.5 ± 5.7	"		19
pCa 5.9	11.7 ± 5.8	"		6

The lower ratio at pCa 5.9 may be due to rigor in the core of the fiber which can occur at saturating [Ca^{++}]. Partial rigor cannot be the explanation for the observed differences between normalized ATPase at pCa 6.4 and 6.8 since rigor would decrease the ratio at the lower pCa. Partial activity of SR may remain in the segments after glycerination. Its contribution to ADP production is being studied.

Our finding that the ratio ADP/∫Pdt-mm is calcium dependent is consistent with the suggestion the Ca^{++} mediates both the number of crossbridges activated and crossbridge turnover rate. (NSF Grant GB-42750)

TH-PM-A4 STEADY AND PRE-STEADY CONTRACTION KINETICS OF CHEMICALLY-TREATED RABBIT PSOAS FIBERS. Jagdish Gulati, National Institute of Arthritis, Metabolism, and Digestive Diseases, NIH, Bethesda, MD 20014.

We exposed fiber bundles from rabbit psoas for 3-5 minutes at 10°C to a solution containing 2.5 M glycerol, 4 mM ATP, 105 mM KCl, 0.75 mM $MgCl_2$, 4 mM EGTA and 7.5 mM imidazole and on return to glycerol-free solutions found that the fibers were permeable to substances in the bathing solution. The treated fibers could be activated by Ca and relaxed by EGTA (pCa = 8). At pCa = 5.0, the force developed by the fibers increased in each successive activation for the first 2 or 3 cycles and then remained constant for 30 or more cycles. The contraction kinetics of these fibers were measured at different temperatures and ionic strengths. Force developed was sensitive to temperature (Q_{10} > 4) in the range 3-15° C. Above 15°C, the force was constant. Isotonic presteady and steady motions were similar to that in the frog except that the rabbit fibers were much slower. V_{max} in rabbit was about 1/10th the value in frog, and the null times (τ, PNAS, 71, 1516, 1974) were 2-3 times as long. Lowering the temperature slowed the isotonic motion as in the frog. For moderate relative load steps, at 3°C, it was found that near the end of the rapid shortening phase of the presteady motion (marked by the time α, ibid) fibers stretched for a brief period of time before shortening again. Effect of ionic strength was similar to that in the frog. At 5°C lowering the KCl from 140 to 75 mM, raised the force without affecting the velocity. Amplitude of the presteady motion was greatly depressed. The rabbit fibers being slower than frog fibers offer a potential for studying the transients with greater resolution. The preparation may also be useful in determining the X-ray diffraction patterns of activated fibers.

TH-PM-A5 CONTRACTILE REPRIMING OF FROG DENERVATED SINGLE MUSCLE FIBERS. S. C. Stuesse* and B. D. Lindley, Dept. of Physiology, School of Medicine, Case Western Reserve University, Cleveland, Ohio 44106.

Following conditioning maximal K^+ contractures of isolated single muscle fibers from Rana pipiens, a brief recovery period is required to restore the ability to produce maximal tension in response to subsequent test depolarization. At 2.5 mM K^+, there is a lag time of 5 sec before any tension can be produced, and recovery is half complete at 13 sec. The time for half recovery is increased by decreasing external $[Ca^{++}]$ and is proportional to the square of the fiber radius. The steady state of recovery depends on the $[K^+]$ during the recovery interval (Na-free tris-methanesulfonate solutions):

Peak tension of test 100 mM K^+ contracture relative to conditioning contracture

$[K^+]$, mM:	7.5	8.75	10	13.75	15
Denervated	.78	.68	.59	.47	.11
Control	.86	.80	.74	.70	.48

There was no significant difference in rate of repriming between normal fibers and fibers which had been denervated for periods of up to 8 weeks. Supported by grants from the USPHS (NS-23016, NS-10196) and the American Heart Association, Northeast Ohio Chapter, Inc.

TH-PM-A6 A STUDY OF FORCE-LENGTH RELATIONS IN NORMAL AND STRETCHED GLYCERINATED RABBIT PSOAS MUSCLE, C. Tyler Burt, Dept. of Biological Chemistry, University of Illinois at the Medical Center, Chicago, Illinois 60612.

The force-length curves (total, passive and active) were examined for both stretched (15 and 30%) and unstretched glycerinated rabbit psoas fibers. The curves were determined for a series of muscles released from one isometric state to another while continuously immersed in contracting solution, i.e., uncycled except for the initial stretches. It was found that unstretched curves behave exactly as do curves for live muscles in that they have almost the same modulus on extension as during shortening. Stretched muscles, though, confirm the results of Edman that the active force in the realm of relative lengths greater than 1.0 is not a linear function with a negative slope and intercept equal to the point of zero overlap. Rather, the force is nearly constant when the passive force is subtracted. In addition, the initial isometric force is almost constant. This is what one would expect from a stable collection of sarcomeres each of which obeys a conventional force-length curve. This situation is then contrasted with live muscle preparations. (This work supported by the Muscular Dystrophy Associations of America and Canada.)

TH-PM-A7 MUSCLE ACTIVATION: THE EFFECTS OF SMALL LENGTH CHANGES ON CALCIUM RELEASE IN SINGLE MUSCLE FIBERS. A.M. Gordon and E.B. Ridgway, Department of Physiology and Biophysics, University of Washington, Seattle, Washington 98195 and Department of Physiology, Medical College of Virginia, Richmond, Virginia 23298.

Small length changes can affect both calcium release and tension in single muscle fibers from the barnacle, Balanus nubilus, depolarized with a constant current. Ca release, measured with the luminescing Ca indicator, aequorin, microinjected into single cells, is less at shorter muscle lengths than at longer lengths. This change can be as much as an 80% decrease in peak light output for a 1% decrease in muscle length or a 30% increase for a 1% increase in length. Over some ranges of muscle length, this change in calcium release with length can account in large measure for the length dependence of the peak isometric tension. The effects of length on calcium release diminished with time such that the greatest effect occurs if the length change immediately preceds the stimulation. For a given current, the muscle fiber membrane depolarizes more at the longer muscle lengths than at the shorter muscle lengths. If the fiber is stimulated with a constant depolarization (voltage clamped), the length dependence of the calcium transient is virtually eliminated. This implies that the effect of length is on a membrane parameter(s) which affects membrane depolarization produced during a constant current and not the direct relationship between membrane depolarization and Ca release. The existence of clefts and extensive invaginations in the surface membrane in these large single muscle fibers may contribute significantly to the length-dependent membrane properties. (Supported by USPHS grants NS08384 and NS10919.)

TH-PM-A8 TENSION TRANSIENTS IN EXTRACTED RABBIT HEART MUSCLE PREPARATIONS. Gerhard J. Steiger* Dept. of Physiology II, Universitat Heidelberg, D-6900 Heidelberg, Germany, and Cardiovasc. Res. Lab. UCLA Med. Center, Los Angeles, Ca 90024.

The tension changes resulting from the application of quick stretches and releases to extracted heart muscle preparations of rabbit have been studied at various amplitudes of length change. The tension changes were analysed as a sum of two exponential processes. After both stretch and release there was first a phase of recovery of tension towards its value before the length change. The rate constant of this phase was fairly sensitive to the amplitude of stretch, increasing from 10 sec^{-1} at 0.3% ΔL to 40 sec^{-1} at 1.5% ΔL at 22°C. On the other hand, the speed of the tension recovery was relatively insensitive to the amplitude if the muscle was released. This amplitude dependence of the quick recovery phase in rabbit heart muscle is the opposite of the amplitude dependence of the rate constant for the quick recovery phase of living frog muscle as published by Huxley and Simmons (1971). In heart muscle the tension recovery was followed by a change in the opposite direction, the delayed rise or fall of tension as described earlier (Steiger 1971). The current interpretation is that the fast tension recovery phase is due to the detachment of crossbridges which are distorted because they were attached at the time the length change was applied. Their force and detachment rate may change as a consequence. On this assumption the extrapolation to zero length change gives an estimate of the rate constant of detachment under isometric conditions. The further tension changes may be a reflection of the approach to a new equilibrium with a rate constant which is the sum of the attachment and detachment probabilities of the undistorted bridges.

TH-PM-A9 CONTROL OF RESTING AND CONTRACTED LENGTH OF CARDIAC CELLS BY INTERNAL LOADS. S. Winegrad, Dept. of Physiology, University of Pennsylvania, School of Medicine, Philadelphia, Pennsylvania 19174.

The range of length over which a myocardial cell operates during its contractile cycle greatly influences the tension it produces, the velocity at which it shortens and the shape of the heart at any given volume. The importance of internal loads in determining the dimensions of cardiac cells has been examined by comparing the sarcomere lengths in resting and activated single cells from frog atria where the tissue organization has been mechanically disrupted with those in the intact trabeculae. In the intact trabeculae the unloaded sarcomere length varies between 1.89 and 2.30μ, but in either single cells or myofibrils the range is 2.1 - 2.2μ indicating the presence of compressive and extensive forces in the intact trabeculae. Electrical stimulation of the intact trabeculae under conditions where 20% of maximum tension is produced causes sarcomere shortening to 1.5 - 1.6μ, but a similar degree of activation of individual cells or myofibrils produces sarcomere shortening to about 1.1μ indicating the presence of a load that is dependent on organization of the tissue. In view of both the transverse and longitudinally oriented collagen fibers in the trabeculae, connective tissue is a likely source of these internal loads.

Supported by grants from U. S. P. H. S. and American Heart Association.

TH-PM-A10 SARCOMERE LENGTH DEPENDENCE OF RESTING AND ACTIVE TENSION OF SKINNED CARDIAC CELLS. A.Fabiato and F.Fabiato*. Harvard Medical School and Peter Bent Brigham Hospital, Boston, Mass. 02115.

Skinned cardiac cells (10μ width, 50μ length) were obtained by homogenization and microdissection of rat ventricular tissue. Tension was recorded with a photodiode force transducer. Sarcomere lengths (SL) were measured on photo-micrographs (resolution 0.2μ). A significant resting tension was observed for a SL 2.1μ; it increased slowly for SL 2.1-2.4μ and very rapidly for SL 2.4-2.7μ. Destruction of the sarcoplasmic reticulum (SR) bythe detergent Brij.58 decreased the tension observed for SL between 2.1 and 2.4μ but not for SL between 2.4 and 2.7μ. It was concluded that the large resting tension observed in intact cardiac muscle is related mainly to the structure of the myofilament lattice.

After measuring resting SL at a pCa 9.0, tonic active tensions were elicited by perfusion at pCa 5.0 in the presence of 4.0mM total EGTA. Maximum tonic tension was observed at SL 2.3μ and 75% of maximum tension at SL 1.5μ. Cyclic contractions were elicited by perfusion with 0.050mM total EGTA at pCa 7.0. They were attributed to a Ca^{2+}-triggered release of Ca^{2+} from the SR. Their amplitude was maximum at SL 2.3μ and was 0% at SL 1.5μ. Phasic contractions were elicited by releasing Ca^{2+} from the SR with 10mM caffeine. The SL-tension curve for these contractions was intermediary between the curves obtained for the Ca^{2+}-triggered cyclic contractions and for the tonic tensions. In rat papillary muscles, the curve of twitch tension vs length was similar to the curve of Ca^{2+}-triggered contractions vs SL in skinned cardiac cells. It was concluded that the rapid fall of tension observed when SL was decreased below optimum in intact cardiac muscle was mainly due to an increase of Ca^{2+} sequestration and a decrease of Ca^{2+} release by the SR at short SL.(A.F. is an E.I. of the Am.Heart Assn.)

TH-PM-A11 EFFECTS OF MAGNESIUM ADENOSINE TRIPHOSPHATE ON SUBMAXIMAL CALCIUM ACTIVATED TENSION IN SKINNED CARDIAC CELLS. P.M. Best* and W.G.L. Kerrick, Dept. Physiol. & Biophys., Univ. Wash. Sch. Med., Seattle, Wash.

Ca^{2+}-activated isometric tension in mechanically skinned rat ventricular fibers was measured in solutions containing $3X10^{-5}$ M, $1X10^{-4}$ M, $1X10^{-3}$ M, and $2X10^{-3}$ M free $MgATP^{2-}$. In addition all solutions contained 7 mM EGTA, 70 mM K^+, Cl^-, 50 μM Mg^{2+}, 15 mM creatine phosphate, creatine phosphokinase, imidazole and varying amounts of Ca^{2+} (pH=7.0, ionic strength=0.15 M, T=21° C). For each [$MgATP^{2-}$] the mean percent of maximum tension was plotted vs pCa and sigmoid curves were fit using the Hill equation. Increasing [$MgATP^{2-}$] shifted the pCa vs percent maximum tension relationship in the direction of increasing Ca^{2+} required for activation. The pCa which produced 50% of maximum tension was 5.8, 5.3, 5.4, 5.5 for the $3X10^{-5}$ M, $1X10^{-4}$ M, $1X10^{-3}$ M, and $2X10^{-3}$ M $MgATP^{2-}$ solutions. The Hill coefficients (1.19, 1.24, 2.20, 2.99) and the steepness of the curves increased as the [$MgATP^{2-}$] was elevated. This change in steepness accounts for the slightly lower [Ca^{2+}] needed for half-maximum tension as the [$MgATP^{2-}$] is increased to millimolar levels. The shift in the pCa vs percent tension relationship as [$MgATP^{2-}$] is changed from $3X10^{-5}$ M to $1X10^{-4}$ M is consistent with the hypothesis of Weber and co-workers that a critical number of rigor bridges can affect the regulatory properties of troponin. The increases in slope at higher $MgATP^{2-}$ levels suggest that even in the absence of rigor bridges the Ca^{2+} sensitivity may be affected by the formation of a critical number of force generating bridges. Supported by PHS grants GM00260 and HL13517. P.M.B. is a Research Fellow of the Wash. State Heart Assn.

TH-PM-A12 Mg^{2+} EFFECTS ON CARDIAC MYOFIBRILLAR ACTIVATION. J.S. Shiner* and R.J. Solaro, Department of Physiology, Medical College of Virginia, Richmond, Virginia 23298.

pCa versus ATPase and calcium binding of purified heart myofibrils was measured in 2 mM MgATP at pMg 4.4, 3.0 and 2.0. Concentrations of all known complexes and ionic species at pH 7.0, 25° were calculated by the Newton-Raphson Method employing Gauss-Jordan Reduction. Because of ambiguity introduced by spurious changes in ionic strength when altering the pMg, the ionic strength was carefully adjusted to 0.1M with KCl. ATPase activity was half-maximal at pCA 6.13 in pMg 4.4, at pCa 5.72 in pMg 3.0 and at pCa 4.99 in pMg 2.0. Hill plots of the relation between pCa and myofibrillar ATPase at varying pMg revealed evidence that Mg may alter the cooperative response to Ca++ activation as measured by the slope of the Hill Plot. These data suggest that Mg may alter interactions between troponin units. At saturating pCa myofibrillar ATPase approximately doubled as the pMg was decreased from 4.8 to 2.8. At pCa 5.0 and pMg 4.4 myofibrils bound approximately twice the calcium bound at pCa 5.0 and pMg 3.0. In the absence of MgATP calcium binding by myofibrils was increased over that in the presence of MgATP at all pCa's studied.

TH-PM-A13 COMPLEX STIFFNESS OF ACTIVATED SINGLE CRAYFISH MUSCLE FIBERS. M. Kawai* and P. W. Brandt, Depts. of Neurology and Anatomy, P & S, Columbia University, New York, New York 10032.

An on line computer controlled apparatus is being used to vary the length of single fibers sinusoidally (0.25 to 133 Hz) and simultaneously measure fiber length and tension. The compliance of the strain gauge is 4 μ/g and signal averaging is used to reduce the tension noise level to RMS 0.3 mg. Distortion of the wave form is 5% according to harmonic analysis, thus the linearity is 99.9% under experiment conditions (ΔL=0.25%Lo). Second harmonic distortion becomes dominant at higher amplitudes and noise increasingly dominates at lower amplitudes. Data from intact crayfish fibers activated by K or caffeine under various ionic conditions were analyzed for complex stiffness by Fourier expansion formulae. This yielded the following 3 distinctive time components: (a) an exponential lead of 160 msec, (b) an exponential delay of 6 msec, and (c) a second lead of 2 msec. Component (b) which represents work by the muscle on the length driver decays with time more rapidly than tension while (a) and (c) persist approximately as long as tension. At its maximum (b) resembles the stretch activation response of the glycerinated insect muscle. In skinned crayfish fibers activated by CaEGTA (1 Mg, 5 ATP) component (b) is absent or very small in amplitude; (c) is 10-fold slower than in the intact fiber and becomes faster as substrate concentration is increased. We propose that component (c) is a measure of the dissociation of actomyosin by substrate and (b) reflects the energy transduction stroke of the cross-bridges.

TH-PM-A14 STRESS-STRAIN BEHAVIOR OF GLYCERINATED CATCH MUSCLE. J.E. Hartt* and W.H. Johnson, Dept. of Biology, Rensselaer Polytechnic Inst., Troy, N.Y. 12181

The glycerinated anterior byssus retractor muscle (ABRM) of *Mytilus edulis* evinces elastic modulus changes with various parameters such as pH, ionic strength, and temperature, which mimic the behavior of the living preparation and molecular paramyosin. We have studied the effect of temperature on phasic and catch-like contractions on the glycerinated preparation and have found that, in this system also, temperatures above 25°C destroy the stretch resistance which occurs in low pH (6.0-6.2) solutions in ATP-EGTA relaxing medium. Calcium-activated actomyosin contractions are unaffected. Low temperatures (to 0°C) have no effect. DeZwaan (PhD Thesis, Utrecht Univ., 1971) has proposed an anaerobically active system for *Mytilus* whereby endproducts such as alanine and succinate are the primary sinks for carbohydrate catabolism. Also formed is D-lactate, which we have found to effect an increase in elastic modulus similar to that caused by lowered pH. Ionic strength has been shown to alter solubility and aggregation characteristics of molecular paramyosin. Similarly, the glycerinated ABRM undergoes a decrease in elastic modulus with increasing ionic strength (0.2 to 0.4). The magnitude of the difference in stretch resistance values from high to low pH, however, increases with increasing ionic strength. The results indicate that actomyosin alone is not responsible for the catch state, but perhaps paramyosin. We also feel that the glycerinated model is a viable tool for studying catch.

TH-PM-B1 MYOSIN FILAMENT STRUCTURE, F. A. Pepe, P. Dowben*, F. Reingold.* Department of Anatomy, University of Pennsylvania, Philadelphia, Pa. 19174

Two models have been proposed for the myosin filament. In one model the myosin molecules are all in parallel and are packed so that the shaft of the filament has a triangular cross sectional profile (Pepe, F. A., J. Mol. Biol. 27, 203-225, 1967). This model predicts that in cross sections of the filament, as the section thickness increases the triangular profile of the shaft will be enhanced and the subunits representing the structural units in the model will become more prominent. In the other model the myosin molecules are "tilted both towards and around the filament axis" (Squire, J. M., J. Mol. Biol. 77, 291-323, 1973). Therefore, this model predicts that as the section thickness increases a circular cross sectional profile will be observed and no subunit structure will be visible. Using a JEM 200KV electron microscope we have observed 2000 Å thick sections. The triangular cross sectional profile of the filaments is clearly observed along the entire length of the filament and the subunit structure of the filament is enhanced. These observations clearly favor the model proposed by Pepe and cannot be explained by the model proposed by Squire. In preliminary optical diffraction studies on thick cross sections we are able to pick up the subunit spacing in the cross section of the filament. The center-to-center distance between subunits is about 37 Å, consistent with previous measurements made from enlarged electron micrographs (Pepe, F.A. and Drucker, B., J. Cell Biol. 52, 255-260, 1972).

TH-PM-B2 FLUORESCENCE CHANGES ASSOCIATED WITH DONNAN POTENTIAL CHANGES IN THE THICK FILAMENTS OF MUSCLE. S.P.Scordilis* Department of Biological Sciences, State University of New York at Albany, Albany, New York 12222.(Intr. by S.L.Izzard)

The fluorescence of the electrofluorochrome CC-6 (3,3'-dihexyl-2,2'-oxacarbocyanine) in the presence of rabbit striated muscle myofibrils has been shown to change linearly with the magnitude of the presumed Donnan potential of glycerol-extracted rabbit striated muscle (Scordilis et al., Proc.Natl. Acad.Sci.U.S., In the press, 1975). Experiments have been performed with synthetic thin filaments (polymerized G-actin (TNF)) and synthetic thick filaments (polymerized myosin (TKF)), to determine how much of the fluorescence change found in myofibrils is due to these proteins. Addition of salt to the synthetic filaments, which should decrease the Donnan potential, decreased the fluorescence of CC-6 with TKF, but not with TNF. The addition of MgATP significantly decreased the fluorescence of CC-6 with TKF. Previously, a similar decrease was found with myofibrils. No such change was seen with TNF. The fluorescence changes of CC-6 with the combination of TKF and TNF were identical to those of the TKF alone. Therefore, the changes in fluorescence and presumably the changes in the Donnan potential occur only in the thick filaments and are independent of the presence of actin.
Supported by Grants NS-07861 and GM-02014 from the U.S.P.H.S. and BC-161 from the Am. Cancer Soc. Inc. The CC-6 was the gift of Alan S. Waggoner of Amherst College.

Biophysical Journal vol. 15, 1975 156a

TH-PM-B3 X-RAY DIAGRAMS FROM GLYCEROL-EXTRACTED RABBIT SKELETAL MUSCLE IN THE PRESENCE OF AMP-PNP. R. W. Lymn and H. E. Huxley‡ NIH, Bethesda, Maryland 20014, and MRC Laboratory of Molecular Biology, Cambridge, England.

When glycerol-extracted rabbit skeletal muscle is bathed in a solution of AMP-PNP (adenylyl-imidodiphosphate) and excess magnesium, it gives rise to X-ray diffraction diagrams that are different from the patterns characteristic of either relaxed muscles or rigor. At 0°, pH 8.0, the cross-bridge pattern typical of rigor is almost completely abolished and there is a considerable increase in the intensity of the meridional reflections (144 and 72 Å) thought to come from the thick filament backbone. The ratio of the equatorial intensities (I_{11}/I_{10}) also changes (by a factor of about two) but does not approach the value typical of live relaxed muscles. At 20° muscles in the presence of AMP-PNP give patterns that are almost completely rigor-like. The results suggest that AMP-PNP acts to weaken the actin-myosin bond, allowing the muscle to give some signs of relaxation (including a drop in stiffness upon stretch), but it does not restore the muscle to the relaxed state.

TH-PM-B4 POLARIZED FLUORESCENCE FROM (CIRCULARLY RANDOMIZED) HELICES. Robert Mendelson, C.V.R.I., University of Calif., San Francisco 94143

Experimental and theoretical investigations of the efficacy of using polarized radiation from extrinsic fluorescent probes as an absolute indicator of changes in helical orientation have been initiated with the aim of applying this sensitive technique to the problem of muscle crossbridge orientation. Previously fits were sought to data assuming emitted fluorescence arose from a system with a randomly distributed fraction and a helical fraction in a proportion determined by trial and error (Tregear and Mendelson---submitted). It was assumed that the dye environments of each fraction were identical. I have found that by considering the distribution of polarized intensities with angle (azimuthial and declination) far more information may be obtained. In particular, for immobile dyes with coincident absorbtion and emission axes an exact expression exists which allows determination of the fractions and the dipole orientation within the helix. It was found that in certain configurations the contribution of the random components to the polarization anisotropy vanish. These predictions for angular distributions of emitted intensity also provide an independent check on the applicability of this model to the system under consideration. A precision polarization goniometer has been constructed to test these predictions. Preliminary results with 1,5 IAEDANS labelled S-1 decorating glycerinated psoas fibers indicates that the model provides an adequate description of the data. Predictions about other models will be discussed and data from directly labelled fibers will be presented.

This work was supported by U.S.P.H.S. Grant Nos. HL 0-6285, HL-1683-01 and N.S.F. Grant No. 24992X.

TH-PM-B5 EFFECTS OF TEMPERATURE AND PRESSURE ON MYOSIN ATPASE OF A BENTHIC FISH. S. Lansman, R. Lukasiewicz, D.J. Hartshorne, and P. Dreizen. Department of Medicine and Biophysics Program, State University of New York Downstate Medical Center, Brooklyn, New York, and Departments of Chemistry and Biology, Carnegie Mellon University, Pittsburgh, Pa.

Studies were conducted on the effects of pressure and temperature on Ca-ATPase and EDTA-ATPase of myosin isolated from white skeletal muscle of benthic fish, Antimora Rostrata, which were recovered from a depth of 2,000 meters, where ambient pressure is approximately 3,000 psi and temperature is approximately 2°C. The temperature profile of myosin ATPase shows thermal denaturation at temperatures greater than 25°C, and a non-linear Arrhenius plot at temperatures less than 25°C, such that temperature-sensitivity is diminished at lower temperatures. The Arrhenius plots for myosin ATPase are non-linear at low substrate (33 μM ATP) and high substrate (3.3 mM ATP), indicating that substrate binding and activation of myosin ATPase, respectively, are involved in the characteristic temperature sensitivity of Antimora myosin. Effects of pressure on myosin ATPase at 4°C are complex, in that at high substrate Ca-ATPase is activated by pressure, whereas EDTA-ATPase is slightly diminished by pressure. However, at low substrate, Ca-ATPase and EDTA-ATPase are essentially invariant to changes in pressure over the range from 1,000 psi to 4,000 psi. The overall data indicate a decrease in temperature and pressure sensitivity of Antimora myosin ATPase, under ambient conditions of 4°C and 3,000 psi, at low substrate, consistent with some kind of adaptation at the molecular level to the unique physiological conditions encountered by Antimora.

TH-PM-B6 EFFECTS OF TEMPERATURE AND PRESSURE ON ACTOMYOSIN ATPASE OF A BENTHIC FISH. R. Lukasiewicz, S. Lansman, D. J. Hartshorne, and P. Dreizen. Department of Medicine and Biophysics Program, State University of New York Downstate Medical Center, Brooklyn, New York, and Departments of Chemistry and Biology, Carnegie Mellon University, Pittsburgh, Pennsylvania.

Enzymatic studies are described of natural actomyosin (containing Ca-sensitive troponin and tropomyosin), as isolated from white skeletal muscle of the benthic fish Antimora Rostrata. At high substrate (3.3 mM ATP), Mg-ATPase exhibits thermal denaturation at temperatures above 20°C, and a decrease in temperature-sensitivity at lower temperatures, such that ΔH^+ is approximately 6 kcal/mole at 4°C. In the presence of EGTA, Mg-ATPase shows comparable thermal denaturation above 20°C; however, at lower temperatures, a marked temperature-sensitivity yields ΔH^+ values as high as 39 kcal/mole. Thus, CA-sensitivity is approximately 10 to 20-fold at 4°C, and 1 to 2-fold at 20°C. At low substrate (33 μM ATP), Arrhenius plots of Mg-ATPase and EGTA-ATPase are essentially similar, with diminished temperature sensitivity from 20°C to 4°C. With respect to pressure effects, at high substrate levels, specific ATPase shows negligible pressure sensitivity over the range of pressure from 500 psi to 3,000 psi; but at higher pressures (8,000 psi), specific ATPase is diminished, at least in part irreversibly. At low substrate, specific activity is augmented by increase of pressure above atmospheric pressure, although pressure sensitivity is negligible over the range from 500 psi to 3,000 psi. The overall data indicate augmentation of specific activity, relative temperature and pressure invariance, and Ca-sensitivity under the ambient conditions of temperature and pressure encountered by Antimora. These findings would be consistent with a molecular adaptation of the actomyosin regulatory system of Antimora.

TH-PM-B7 EFFECT OF CREATINE AND CREATINE ANALOGS ON CREATINE KINASE SYNTHESIS IN DIFFERENTIATING SKELETAL MUSCLE IN VITRO. J.S. Ingwall, N.F. Hall* and G.L. Kenyon*, Univ. of Calif., San Diego, La Jolla, CA 92037 and Univ. of Calif., San Francisco, San Francisco, CA 94143.

Increasing the concentration of creatine (Cr), an end product of contraction, available to differentiating skeletal muscle cells in culture selectively stimulates the rates of synthesis of myosin heavy-chain and actin ∿100%. Cr stimulation of contractile protein synthesis is supported by measurement of the activities (units/mg protein) and isoenzyme compositions of creatine kinase (CPK), some of which is localized in the myofibril, and lactic dehydrogenase (LDH), a glycolytic enzyme. The activities of both enzymes increased with time in culture and the percent of muscle-type isoenzymes increased after cell fusion was essentially complete. Between day 2 and day 7 in culture, the specific activity of the non-muscle form of CPK (BB-isoenzyme) did not change, while the muscle-type isoenzyme (MM-isoenzyme) increased 8-fold. In Cr-supplied cultures, CPK activity was enhanced (134±4% of control, n=32, $p<10^{-6}$). Cr did not affect the amount of BB-isoenzyme present in the cultures but did stimulate the synthesis of MM-isoenzyme two-fold. Several Cr-analogs were also tested for their ability to substitute for Cr in stimulating MM-CPK synthesis. Analogs similar to creatine (high relative Vmax) such as 1-carboxymethyl-2-iminoimidazolidine substituted for Cr in stimulating MM-CPK synthesis while poor analogs (low relative Vmax) such as N-methyl-amidino-N-methylglycine suppressed MM-CPK synthesis. In contrast, creatine does not affect LDH activity (99±2% of control, n=32) or LDH isoenzyme composition. These results support the observation that Cr selectively stimulates myofibrillar protein synthesis. (Supported by NIH Contract Award NOL-HL-81332).

TH-PM-B8 FURTHER CHARACTERIZATION OF ALPHA PARAMYOSIN: REDUCED VS. OXIDIZED FORMS. Jacqueline P. Merrick and William H. Johnson, Biology Dept., Rensselaer Polytechnic Inst., Troy, N.Y. 12181

It is now generally accepted that alpha paramyosin, a molecule which appears to be about 5% larger than the classical ethanol prep extracted from Mercenaria mercenaria, is the native paramyosin species. Cowgill has recently reported that Mercenaria paramyosin contains four cysteine residues, most likely two per chain. These exist in vivo in the reduced form (Cowgill, R.W.(1974), Biochem. 13, 2467). Extraction of paramyosin in the presence of dithiothreitol as well as EDTA protects the sulfhydryl groups from oxidation. Our studies indicate that alpha-reduced (R)-paramyosin differs from the oxidized form in several respects. Alpha-R-paramyosin is generally more soluble than alpha-oxidized over an ionic strength range from 0.2 to 0.45M. However, its phase change from monomer to aggregate is more abrupt and occurs between 0.35-0.25M, at pH 7. When ionic strength is held constant at 0.35M, and the pH is decreased from 7.0 to 6.7, alpha-R-paramyosin solubility falls off at a more rapid rate than that of the oxidized form. Certain molluscs accumulate lactate as a metabolic end product of the glycolytic scheme. In the presence of 50 mM lactate at pH 7.0, alpha-R-paramyosin begins to aggregate at a higher ionic strength than the control without lactate, forming large birefringent needles, as observed in phase contrast microscopy. These studies suggest that alpha-R-paramyosin is a physiologically poised system. Conformational changes in the thick filament paramyosin core, possibly leading to the catch state, could occur as a result of very small changes in pH, ionic strength, and/or the presence of certain metabolites such as lactate.

TH-PM-B9 EVIDENCE FOR SIMILARITY AMONG MOLLUSCAN AND ARTHROPODAN PARAMYOSINS. R. Levine, M. Elfvin and M. Dewey. The Medical College of Pennsylvania, Philadelphia, Pa. 19129 and SUNY at Stony Brook, N.Y. 11790.

Heterogeneity among paramyosins (PMs) extracted from different invertebrate species has been assumed on the basis of differences in their molecular weights. One explanation proposed for such variability is that degradation of polypeptide chains sometimes occurs during extraction yielding fragments smaller than the intact molecules (Stafford and Yphantis, Biochem. Biophys. Res. Comm. 49:848, '72). We have calculated the polypeptide chain weights of PMs of isolated myofibrils from several arthropodan and molluscan muscles using SDS-polyacrylamide gel electrophoresis. All of our gels show a band with the mobility of purified Limulus PM (chain weight: 115,000±4,000 daltons) isolated by the method of de Villafranca and Haines (Comp. Biochem. Physiol. 47B:9, '74). On the other hand, Mercenaria PM, prepared by the method of Johnson et al (Science 130:160, '59) has a greater mobility in our gels than either purified Limulus PM or the myofibrillar PMs and appears as two bands with chain weights of ∿102,000 and ∿97,000 daltons, similar to the reported proteolytic fragments. Addition of Limulus PM to gels of muscle homogenates, including Mercenaria, enhances only the endogenous PM bands, while addition of Mercenaria PM to the Mercenaria gels only creates the two new bands described above. This demonstration of identical chain weights of non-extracted PMs suggests a fundamental similarity among them. This is supported by their immunologic cross-reactivity, shown by A band staining of a variety of invertebrate muscles using PAB-cellulose purified antibody specific for Limulus PM. Supported by a grant from The Arcadia Foundation, USPHS Grant GM20628 and USPHS Grant HL15835 to the Pennsylvania Muscle Institute. R.L. was awarded USPHS RCDA K04 NS 70476.

TH-PM-B10 ACTIN-LINKED CALCIUM CONTROL IN NON-MUSCLE CYTOPLASM V. Nachmias* and A. Asch*, Department of Anatomy, University of Pennsylvania, Philadelphia, 19174 (Intr. by R. E. Davies)

A pellet of "ground cytoplasm" est'd as 30-40 S components and prepared from 100,000 g 1 hr supernatant of a low salt extract of Physarum has been studied and similar preliminary results obtained with human platelets. The pellet fraction has little endogenous ATPase activity but in 0.05 M KCl has 1.5 to 8 fold (different preparations) greater MgATPase in 0.1 mM free calcium as compared to 1 mM EGTA. EGTA inhibition is released by added desensitized rabbit actin as a function of added actin. Double reciprocal plots show near or complete (different preps.) reversal of EGTA inhibition at infinite actin. Several criteria including the use of myosin-specific anti body show conclusively that actin and myosin are in the pellet fraction. When muscle (VStrM) myosin was added to the high speed supernatant and recollected, a "hybrid actomyosin complex" was formed in which several new proteins coprecipitated. The 1.5-3 fold calcium sensitivity of the hybrid was lost on washing and could be restored with concentrated washate in conjunction with loss and restoration of several bands on SDS gels; these were impure but contained bands at 55,000 daltons and also in the 18,000-39,000 range. We conclude that actin-mediated calcium regulation occurs in Physarum associated with factors which are very easily lost. Purification of the factors using hybrid complexes from non-muscle systems is now feasible.

Support: Grant #AM-17492 and in part HL-15835.

TH-PM-B11 MEMBRANE ASSOCIATED ACTIN: DECREASE FOLLOWING THE TRANSFORMATION OF CHICK EMBRYO FIBROBLASTS. Eric Gruenstein, Gary Wickus*, and Alexander Rich, College of Medicine, University of Cincinnati, Cincinnati, Ohio, Gunderson Clinic, Onalaska, Wisc., and Biology Dept., MIT, Cambridge, Mass.

Membranes prepared from cultured chick embryo fibroblasts contain a component which co-migrates with chick skeletal muscle actin on polyacrylamide gels. This presumptive actin band has been positively identified as actin by tryptic peptide mapping. Following transformation of the cells by Rous sarcoma virus, the amount of actin associated with the membranes is decreased by 30 to 50 percent depending upon whether the membranes are prepared as sheets or vesicles. This result is not due to infection per se, since a temperature sensitive strain of the virus decreases membrane associated actin only at the permissive temperature. A shift from the non-permissive (41°) to the permissive (36°) temperature results in an increase in the percentage of total cellular protein synthesis devoted to actin production so that the decrease in membrane associated actin appears to be due to a selective displacement of actin from the membrane rather than a general decrease in total cellular actin. The possible significance of subcellular actin redistributions will be discussed in terms of the well-known alterations in fibroblast movement and morphology associated with viral transformation.

TH-PM-B12 AN ANALYTICAL MEASUREMENT OF THE STIFFNESS OF INTACT AND DEMEMBRANATED SEA URCHIN SPERM DURING MOTILITY. C.B. Lindemann, Dept. of Biological Sciences, Oakland University, Rochester, Michigan 48063.

Photographs of the sperm of the Pacific Sea Urchin Tripneustes gratilla (provided courtesy of I.R. Gibbons & B.H. Gibbons) were used to measure the bend curvatures of beating sperm flagella. Photographs were selected which displayed the wave form of free swimming sperm and also of sperm which had become attached by their head to the microscope slide. Multiple flash exposures were taken of sperm in a medium containing milk solids. These photographs displayed the motion of suspended particles which resulted from fluid movement caused by the flagella, and were used to calculate the velocity of the fluid moving past the flagellum. Using the beat frequency, the wave form, and fluid velocity data, the propulsive force (i.e. axial component of the drag) acting on the flagellum was calculated. The difference in the bend curvatures between the free and the attached sperm flagella, together with the value of the propulsive force acting on each bend, were used to calculate the effective stiffness of the structure. The procedure was applied to photographs of intact sperm, and reactivated sperm which were demembranated with Triton X-100 (B.H. Gibbons & I.R. Gibbons, 1972, J. Cell Biol. 54:75). The stiffness value obtained for intact cells was $1.5 \times 10^{-13} \pm 0.6 \times 10^{-13}$ dynes cm^2 as compared to a value of $1.4 \times 10^{-13} \pm 0.6 \times 10^{-13}$ dynes cm^2 for demembranated cells. It is concluded that the dynamic (moving) stiffness of the flagellum represents a property of the tubulin axoneme and its accessory protein structures, and is not dependent on the presence of the plasma membrane. (Work was initiated at the University of Hawaii with the help and cooperation of Dr. Ian R. Gibbons and was supported in part by USPHS grant HD-06565).

TH-PM-B13 FURTHER STUDIES ON PHYSARUM MYOSIN. M. R. Adelman. Department of Anatomy, Duke University Medical Center, Durham, North Carolina 27710.

Physarum plasmodia were extracted with TM buffer (.01 M Tris-maleate, .005 M β-Mercaptoethanol, pH 7.0) which preferentially releases actin, leaving myosin in the residue. The plasmodial myosin was then differentially extracted with TM plus .05 M $NaPP_i$ and was highly purified by salt fractionation followed by chromatography, in succession, on Sepharose 6B, hydroxylapatite, and DEAE cellulose. Yields of 5-6 mg myosin were obtained per 100 gm plasmodium, representing 15-20% of the total myosin present. Discontinuous SDS-polyacrylamide gels reveal the enzyme consists primarily ($\geq$ 90%) of an ∿225,000 ± 15,000 dalton polypeptide. Several minor components of lower MW were detected, including a doublet at ∿12,000 daltons. The minor components were not resolved from the enzyme peak (∿6S) in sucrose density gradients and were present in preparations made using various proteolytic inhibitors. Assuming the native enzyme contains two heavy chains and weighs ∿470,000 daltons, some (or all) of the minor components must be contaminants and/or breakdown products; hence, it is not certain whether Physarum myosin contains specific light chains. Physarum myosin is a calcium-dependent enzyme with a specific activity of ∿2.0 μM P_i/mg/min. in .50 M KCl, .005 M $CaCl_2$, pH 8.0. The absence of KCl-EDTA ATPase does not appear to reflect alteration of -SH groups. At low KCl the Mg^{2+}-ATPase of the myosin is strongly activated by Physarum actin; the activation decreases with increasing KCl. At 12.5 mM KCl, 1.5 mM $MgCl_2$, 1 mM ATP, TM, and room temperature, 25 μg/ml myosin is activated 6-fold and 15-fold by 50 μg/ml and 200 μg/ml actin, respectively; double reciprocal plots indicate an activity of ∿1 μM P_i/mg myosin/min. at infinite actin. As yet, no evidence has been obtained for either myosin-linked or actin-linked (Fed. Proc.33: 1522a,1974) calcium-regulation. Supported by NIH grant #'s 5-S04-RR-6148 and 2-R01-GM-20141.

TH-PM-B14 A MODEL FOR HUMAN PLATELET MYOSIN FILAMENTS. R. Niederman* and T. D. Pollard, Department of Anatomy, Harvard Medical School and Harvard School of Dental Medicine, Boston, MA 02115 (Intr. by E.M. Ettienne)

We previously have studied the in-vitro self assembly of purified human platelet myosin. Electron microscopic measurements show that in .1 M KCl at pH 7, platelet myosin forms small bipolar filaments about 320 nm long and 10 to 11 nm wide, while skeletal muscle myosin under identical conditions forms filaments 3 to 5 times longer. We have now derived a general equation which relates several structural parameters of myosin filaments, the size of the myosin molecule and the dimensions of the myosin filament. The equation is particularly useful for calculating the number of myosin molecules with heads in each axial repeat (n) from easily measured dimensions of negatively stained filaments - the length of the bare zone (156 nm), the diameter of the filament in the center of the bare zone (10.5 nm), and the length of the axial repeat (14.5 nm). The number of myosin molecules per filament can then be calculated from the number of myosins per axial repeat and the length of the filament. From these considerations one can construct a model for synthetic platelet myosin filaments which consists of 28 myosin molecules arranged in a bipolar array with the heads of two myosin molecules projecting from the backbone of the filament in each 14 to 15 nm axial repeat (n=2). The transformation of this two-dimensional model into three dimensions requires information about the azimuthal arrangement of the myosin heads. This has been difficult to determine because the heads appear to be loosely attached to the backbone of the filament by flexible connections.

TH-PM-C1 PREDICTED MEMBRANE NOISE SPECTRA DUE TO HODGKIN-HUXLEY SODIUM CHANNEL GATING, W. O. Romine and R. J. Bradley, Neurosciences Program and Department of Physiology/Biophysics, University of Alabama Medical Center, University Station, Birmingham, Alabama 35294

If it is assumed that sodium channel gating is a stochastic process that follows the laws of statistical mechanics and chemical rate theory, then it is possible to predict the power spectrum of membrane noise that is due to the fluctuations from and relaxation to equilibra in membrane sodium currents given a specific model. For a Hodgkin-Huxley model (HH), it can be shown (details to be published) that the m^3h power spectrum is:

$$G(f)=4\gamma I_{Na}(V-V_{Na})\left[\sum_{i=0}^{1}\sum_{j=0}^{3}\binom{1}{i}\binom{3}{j}\frac{h_\infty^{1-i}m_\infty^{3-j}(1-h_\infty)^i(1-m_\infty)^j(i\tau_m+j\tau_h)\tau_m\tau_h}{(i\tau_m+j\tau_h)^2+(2\pi\tau_m\tau_h f)^2}\right]$$

where $ij \neq 0$

γ is the unit channel conductance of one sodium channel and the other terms are the standard HH terms (Hodgkin and Huxley, J. Physiol. 117 (1952) 500). Deviations from this theoretical spectrum might be indicative that the HH process does not represent the correct physical description of sodium channel gating. In particular, a kinetic scheme involving coupled activation-inactivation processes might prove an attractive alternative. NSF predoctoral fellowship support to W. O. R. is acknowledged.

TH-PM-C2 GATING MOLECULES, SO-CALLED "GATING CURRENTS," AND BROWNIAN MOVEMENT IN THE EXCITABLE MEMBRANE. F. F. Offner, Technological Institute, Northwestern University, Evanston, Illinois 60201.

Long-chain ionized molecules, deflected by the radial component of the boundary electric field, can gate ion flow and thereby account for the observed differential permeability changes of Na and K in the axonal membrane. So-called "gating currents" are independent of such molecular movements, but are the expected result of the diffusion of ions within the membrane, their asymmetry resulting from the various asymmetries of the membrane itself, including fixed charge distribution and double layer structure. Calculation of such asymmetric diffusion currents agree generally with the reported "gating currents," which should more properly be termed "intra-membrane diffusion currents."

Brownian movement of the gating molecules contributes a small component to the membrane current noise, but this component should have a substantially flat power spectrum. The major component of noise appears to be due to the randomness of the diffusion of ions into the membrane channels.

TH-PM-C3 INACTIVATION OF GATING CHARGE MOVEMENT. F. Bezanilla and C. M. Armstrong. University of Rochester School of Medicine, Rochester, New York.

We reported previously that inactivation of the sodium conductance (gNa) affects gating current (Ig). We have studied this effect quantitatively by several procedures. i) We determined total gating charge movement during the opening of Na channels (Qg on) for pulses of various durations, and compared this to Qg magnitude during closing of the channels (Qg off) after pulses of the same durations. For short pulses, Qg off and on are equal (off/on ratio =1 or near it), but for long pulses (5 msec at +50mv, 8°C), the off/on ratio falls to about 1/3; i.e., about 2/3 of Qg is apparently immobilized by the inactivation process, and moves back to its original (closed) position so slowly on repolarization that it escapes detection. ii) Prepulses which inactivate gNa decrease Qg on. For a symmetrical pulse pattern with a 1 msec interval between pre and test pulse (8°C) Qg on is reduced to less than half its control value by a prepulse. iii) A prepulse (with test pulse superimposed) reduces Qg movement over the range -70 to +20mv to about 1/3 of its control value. Pronase, which removes gNa inactivation, abolishes the effect of prepulses and prevents the reduction of Qg off with increasing pulse duration. Inactivation significantly alters the distribution of Qg as a function of Vm, reducing Qg movement from -70 to +20mv and steepening the Qg-Vm curve for Vm negative to about -70mv. From these results we infer that activation and inactivation of gNa are not independent processes (though separable by pronase), and that Ig has at least two components, one of which is unaffected by inactivation. (Supported by USPHS Grant NS08951.)

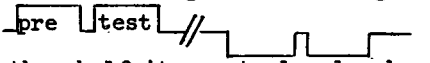

TH-PM-C4 PERFUSION OF THE MYXICOLA GIANT AXON. G. A. Ebert* and L. Goldman, Dept. of Physiology, School of Medicine, Univ. of Maryland, Baltimore, Maryland 21201.

Myxicola giant axons were internally perfused using a modification of the cannulation technique of Tasaki and Watanabe. No outflow cannula was used, and the axon was briefly exposed to 1 mg/ml papain to initiate flow. In normal internal medium (275 mM KF, 1mM NaF, 1 mM Hepes, 485 mM dextrose, pH 7.5 ± 0.05), at 5°C, mean initial action potential (spike) amplitude was 111 mV (range: 105 to 114 mV) and mean initial resting potential (E_m) was -57.8 mV (range: -61.5 to -54.5 mV). The initial spike amplitude was stable (to about 5 mV) reliably for 20-30 min, but could hold up to 1 hr. Preparations remained excitable reliably for 1 to 1.5 hr, but have survived up to 2.5 hr. All spike amplitudes were determined following an 80 msec inward current pulse to a potential of -110 mV to remove inactivation. The relationship between the potential at the spike peak and the internal sodium activity (αNa_i) was well described, over a range of αNa_i from 0.68 mM to 136 mM, by the constant field equation:

$$E = \frac{RT}{F} \ln \frac{\alpha K_o + (P_{Na}/P_K)\ \alpha Na_o}{\alpha K_i + (P_{Na}/P_K)\ \alpha Na_i}$$

where E is potential, P_{Na}/P_K is the sodium to potassium permeability ratio, the subscripts o and i refer to external (artificial sea water) and internal media respectively, and R, T and F have their usual meaning. P_{Na}/P_K was 5.77. E_m *vs* αK_i was also reasonably well described by the constant field equation, with a P_{Na}/P_K of 0.031 (the value fitted to E_m vs. external potassium concentration data in Myxicola).

Supported in part by U.S.P.H.S. grant # NS07734.

TH-PM-C5 THE EFFECT OF CONDITIONING POTENTIAL ON POTASSIUM CURRENT KINETICS IN THE FROG NODE. Y. Palti, R. Stampfli, G. Ganot & G.Ehrenstein, Department of Physiology & Biophysics, Technion Medical School, Haifa, Israel, and the 1st Physiological Institute, Saarlands University, Homburg, Saar.

The potassium conductance time constant, τ_n, was determined in the voltage clamped frog (R. Esculenta) Node, as a function of conditioning prepotential. The conditioning potential duration was varied from 1 to 50 msec and amplitude between -60 and +130 mv (relative to rest). The current kinetics were determined at single test potential of +20mv (depolarization). The values of τ_n following conditioning hyperpolarizations were around 5 msec, 2-4 times greater as compared with values obtained following strong depolarization. These differences were only slightly dependent on $[K^+]_o$ or conditioning pulse duration. The τ_n vs prepotential value curve is sigmoid in shape. Following conditioning hyperpolarizations the log $[n_\infty - n_t]$ vs time curve could not be fitted by a single exponent regardless of the power of n chosen. This prepotential dependency of potassium current kinetics is inconsistent with the Hodgkin-Huxley axon model where the conductance parameters are assumed to be in either one of two possible states, and where the rate of transfer from one state to the other follows first order kinetics. The above potassium kinetics are consistent with a multistate potassium "channel" model.

TH-PM-C6 A FOUR BARRIER MODEL OF THE SODIUM CHANNEL. Bertil Hille, Dept. Physiol. & Biophys., Univ. Wash. Sch. Med., Seattle, Wash. 98195

For nodes of Ranvier, "independence" does not correctly describe changes in peak currents in Na channels as external Na^+ is replaced by TMA^+, Tl^+, Li^+, guanidinium compounds and other Na-substitutes (Hille, J. Gen. Physiol. 58:599, 1971; 59:637, 1972). Deviations occur with pure Na-substitutes or mixtures of Na plus substitutes (Hille in Eisenman "Membranes 3" Dekker 1975). Evidently high concentrations of Na^+ or Na-substitutes block Na channels. As with H^+ ions (Woodhull, J. Gen. Physiol. 61:687, 1973) block depends on voltage and suggests a binding site 25-30% of the way across the membrane and within the channel. Selectivity, competition, and voltage-dependent blocks are well modelled by an Eyring rate theory barrier model solved for the case with only one ion allowed in the Na channel at a time. Barrier s.f. is the "selectivity filter" and valley b.s. is the binding site. Numbers are energies of peaks and valleys for Na^+ ions in multiples of RT (~600 cal/mole). Table gives equilibrium zero-field dissociation constants of b.s. (K_{bs}) and relative energies (units of RT) at s.f. (ΔG_{sf}) and at b.s. (ΔG_{bs}), calling ΔG for Na^+ zero. The binding site may be the site of competition of TTX, STX, H^+, Tl^+, Na^+, etc. By contrast a similar barrier model for blocks in K channels requires solving with single-file movement of several ions within the channel at once.

Supported by PHS grant NS08174.

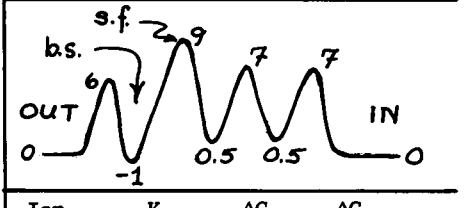

Ion	K_{bs}	ΔG_{bs}	ΔG_{sf}
Na^+	368 mM	0	0
Li^+	165	-0.8	+0.08
Tl^+	50	-2.0	+1.4
OH-guan$^+$	74	-1.6	+2.5
H^+	0.004	-11.4	>-6.8

TH-PM-C7 A DYNAMIC MODEL OF THE SODIUM CHANNEL. M. P. Remler, Division of Neurology, University of North Carolina School of Medicine, Chapel Hill, North Carolina 27514.

The sodium channel is modeled as an aqueous cylindrical pore with inert walls except for charge rings distributed near the middle and hydrated charge blocking the inside opening. The charge rings are two dipoles back to back with the positive charges merged. The equasions of ion diffusion through an aqueous pore with this electric field results in markedly different ion specific conductances. The ion selectivity of the charged rings can be matched quantitatively to the known relative conductances of cations in neural membranes.

The mechanism of sodium conductance changes during voltage clamp experiments and in action potentials is described by nonlinear differential equasions governing the interaction between sodium flux through the channel and the hydrated charge barrier. The density of hydrated charge inside the membrane is the factor controlling the opening and closing of the channel. The ion flux decreases the hydrated charge barrier which causes the positive feedback of further depolarizing sodium current. This continues until the ion flux cannot match the charge dissipation inside the membrane which results in repolarization which results in a return of the hydration barrier and a positive feedback of declining ion flux until the pore closes again. Threshold to depolarization, the time course of sodium conductance, and the refractory periods are quantitatively explained. No macromolecular rearrangements are invoked and the model is compatible with current knowledge of membrane structure.

TH-PM-C8 IONIC SELECTIVITY OF THE SODIUM CHANNEL IN FROG MUSCLE. Donald Campbell* (Intr. by B. Hall). Dept. Physiol. & Biophys., Univ. Wash. Sch. Med., Seattle, Washington 98195

The method of Dodge and Frankenhaeuser (J. Physiol. 180:788, 1958) was modified to study the membrane of frog skeletal muscle fibers under voltage clamp conditions. Resolution was improved over previous attempts to apply this technique to muscle by adapting the frequency response of the amplifiers to the muscle preparation, cutting the ends in isotonic CsF, and electronically subtracting the capacity and leakage currents from the records. Currents in Na channels could be measured starting about 80 μsec after the voltage step and were similar to those of the node of Ranvier. The reversal potential of this current was measured in test solutions with all the external Na^+ replaced by other ions. Permeability ratios for the test ions were computed from reversal potential changes using the Goldman-Hodgkin-Katz equation and are given in the table. Permeability ratios are not significantly different from those measured for the node of Ranvier (Hille, J. Gen. Physiol. 58:599, 1971; 59:637, 1972). As in the node, no inward currents were observed with isotonic Ca^{++} or with small methylated cations. Permeability ratios for these ions were calculated to be smaller than: Ca 0.093, TMA 0.008, TEA 0.008. The results are consistent with the Hille (1972) model of the Na channel selectivity filter of the node and suggest that the selectivity filger of the two tissues is the same. Supported by PHS grants GM00260 and NS08174.

P_{ion}/P_{Na}	Ion
1.0	Na
0.96	Li
0.94	hydroxylamine
0.31	hydrazine
0.11	ammonium
0.093	guanidine
0.048	potassium
0.031	aminoguanidine

TH-PM-C9 TTX-BINDING TO FROG MUSCLE AND THE CONDUCTANCE OF A SINGLE SODIUM CHANNEL. W. Almers* and S.R. Levinson* (Intr. by A.C. Brown). Physiol. Lab., Cambridge CB2 3EG and Dept. Physiol., U. Wash. Sch. Med., Seattle.

Using both bioassay and radioisotope methods, we have examined the binding of tetrodotoxin (TTX) to frog sartorius muscle. This tissue has the advantage of allowing electrical as well as biochemical studies of membrane properties. We find a saturable component of TTX binding with a capacity of about 22 pMoles/g wet and half-saturation at 5 nM. If this uptake represents one-to-one binding of TTX to sodium channels, the channel density in a muscle of 0.3 ml/g extracellular space and 80 μm fiber diameter is about 380/μm^2 referred to unit area of surface membrane. In conjunction with voltage-clamp measurements of muscle sodium conductance, the present result allows one to estimate the conductance of a single sodium channel as about 10^{-12} mho. This is one to two orders of magnitude less than previous estimates obtained from TTX binding on tissues which do not allow measurement of the maximal sodium conductance. Our estimate is also lower than the single channel conductances of the two virtually non-selective cation pores opened by acetylcholine and gramicidin-A. This makes good sense, since one might expect that a channel which does not discriminate between univalent cations, should permit higher transit rates than the relatively selective sodium channel, which first has to "test" each approaching ion before allowing its passage. We also find that maintained depolarization does not measurably affect TTX-binding. This suggests that there is little molecular interaction between the "gating" portion of the sodium channel molecule, and that which binds TTX. Supported by PHS grant AM17803.

TH-PM-C10 SIZE DEPENDENT EFFECTS OF THE LN^{3+} IONS IN SQUID AXON. J. Senft, Juniata College, M. Starzak, SUNY-Binghamton, and W.J. Adelman, N.I.M.D.S.,N.I.H.

McLaughlin, et.al. (PNAS(1970) 67:1268) proposed a "screening" model for the effects of multivalent ions at membrane surfaces. D'Arrigo has observed "screening" for crayfish axon using La^{3+}, Y^{3+} and Eu^{3+}.(J.Physiol. (1973)231:117). To test this hypothesis the effects of a series of Ln^{3+} ions have been studied in the squid giant axon preparation. The Ln^{3+} ions were chosen for their chemical similarity. The ions also exhibit a decrease in ionic radius with increasing atomic number. Since their radii are comparable to that of Ca^{2+} ion, the effects of ionic size, if such effects exist, can be determined. Voltage clamped squid giant axon were bathed in K^+, Mg^{2+} free artificial sea water solutions with 2 or 5 mM Ca^{2+} and 0.1mM La^{3+}, Sm^{3+}, Eu^{3+} or Yb^{3+}. K^+ steady state currents were reduced relative to 5 mM Ca^{2+}standard ASW solutions for a depolarizing pulse of +110 mv. in the proportion

La:Sm:Eu:Yb = 0.89:0.62:0.52:0.23

At a clamping voltage of +110 mv above the holding potential, the corresponding τ_n's increased as

La:Sm:Eu:Yb = 1.7:2.7:2.9:3.2

The Na^+ τ_h's exhibited a similar increase while the Na^+ τ_m's showed little change. This is reflected in an increase in the maximum inward Na^+ current for a depolarizing pulse of +60 mv. The relative increase is

La:Sm:Eu:Yb = 1.06:1.25:1.09:1.53

The Ln^{3+} series shows size dependent effects on the ionic conductance parameters during voltage clamp which are inconsistent with a "screening" model. The increased effects with decreasing ionic radii strongly suggest membrane binding.

TH-PM-C11 THE DOUBLE NEGATIVE RESISTANCE OF EIM AND ITS RELATION TO INACTIVATION IN EXCITABLE MEMBRANES. G. Ehrenstein and H. Lecar, Laboratory of Biophysics, IR, NINDS, National Institutes of Health, Bethesda, Md. 20014.

A positive membrane potential of sufficient amplitude drives EIM channels in oxidized cholesterol bilayers from an open state to a closed state, thus decreasing the membrane conductance. Negative membrane potentials also decrease membrane conductance, and the question can be raised as to whether the channels are driven to the same closed state as for positive potentials or whether there are two distinct closed states. We have determined experimentally that there is a second closed state. To test this point, a large negative potential was followed by a large positive potential. The conductance decreased during the negative potential; during the positive potential it increased and then decreased. This indicates that during the positive potential the channels were driven from the negative closed state to the open state and then to the positive closed state. The conductance kinetics for such a three-state channel offer a possible mechanism for the inactivation of natural excitable membranes.

TH-PM-C12 K^+ CONDUCTANCE NOISE INDUCED BY TEA AND ITS C_{10} DERIVATIVE IN SQUID AXON. H.M. Fishman, L.E. Moore, and D.J.M. Poussart*, Univ. of Texas, Galveston, Tx.; Case Western Reserve Univ., Cleveland, Ohio; Laval Univ., Quebec.

Power-density spectra of current noise from voltage-clamped patches of squid axon membrane were measured under conditions of internal perfusion with standard perfusate (buffered .5M KF) and with 10mM TEA and .1 mM TEA-C_{10} derivative added. Control spectra show a voltage-dependent component characteristic of K^+ channel relaxation (Fishman, PNAS, 70: 876, 1973). The relaxation component disappears from spectra when either (K_i^+) is 50mM or less or in the presence of 10mM TEA. Depolarization of the patch potential during standard perfusion w/TEA produces large excess noise power (100 fold above thermal) and the form of spectra (10-1000Hz) becomes flat with increasing depolarization. In low (K_i^+), with or without TEA, no significant increase in noise power occurs with depolarization. In .1mM TEA-C_{10} and standard perfusate, the noise power also increases with potential similar to TEA experiments; however, in addition, a hump reappears in spectra with a corner frequency which appears to relate to the kinetics of g_K inactivation produced by TEA-C_{10} in patch step-clamp currents. These data suggest that TEA and its C_{10} derivative interact with membrane sites, which affect K conduction, to induce conduction noise associated with their binding kinetics.

Aided by NS 11764 (HMF), NS 08409 (LEM), and A5274 (DJMP)

TH-PM-D1 ACTION SPECTRUM FOR ACTIVATION OF CYCLIC NUCLEOTIDE PHOSPHODIESTERASE IN VERTEBRATE PHOTORECEPTORS. J.J. Keirns*, N. Miki*, M.W. Bitensky*, and M. Keirns* (Intr. by F. Hutchinson), Departments of Pathology and Chemistry, Yale University, New Haven, Connecticut 06510.

Frog (Rana pipiens) rod outer segment disc membranes contain a cyclic nucleotide phosphodiesterase (EC 3.1.4.c) which, in the presence of ATP, is stimulated 5 to 20 fold by illumination. The effectiveness of monochromatic light of different wavelengths in activating phosphodiesterase was examined. The most effective is light of wavelength 500nm. The entire action spectrum from 350 to 800 nm closely matches the absorption spectrum of rhodopsin. Thus, rhodopsin appears to be the pigment which mediates the effects of light on phosphodiesterase activity. Trans retinal alone does not mimic light. Half maximal activation of the phosphodiesterase occurs with a light exposure which bleaches 0.05% of the rhodopsin. Half maximal activation can also be achieved by mixing 1 part of illuminated disc membranes in which the rhodopsin is bleached with 99 parts of unilluminated membranes. This difference in sensitivity found by the two procedures probably reflects the fact that phosphodiesterase interacts more readily with a bleached rhodopsin on the same disc membrane than with a bleached rhodopsin on another disc membrane. These studies show that the levels of cyclic nucleotides in vertebrate rod outer segments are regulated by minute quantities of light and clearly indicate that rhodopsin is the photopigment whose state of illumination is closely linked to the enzymatic activity of disc membrane phosphodiesterase. These findings also represent the first demonstration of coupling of the photoisomerization of rhodopsin to the activity of a specific disc membrane enzyme.

TH-PM-D2 ATP IN RETINAL RODS. W.E.Robinson,† S. Yoshikami† and W.A. Hagins,† N.I.H., Bethesda, Maryland 20014. †NEI †NIAMDD

Suspensions of freshly isolated frog rod outer segments (r.o.s.) have been assayed for ATP in a continuous stream analyzer by the firefly Luciferin-Luciferase (L-L) method. Washed, fresh r.o.s. cause little light emission on mixing with L-L. If previously exposed to Triton X-100, ground in an ultra-sonic mill, or freeze-thawed, ATP is readily detected. The ATP concentration in a sonicated stream containing r.o.s. shows fluctuations consistent with the number of ATP-bearing particles being equal to the number of o.s. with intact plasma membranes [Yoshikami, et al. Science, 185, 1176 (1974)]. The ATP concentration in fresh o.s. cytoplasm ranges from 2-5 mM. In darkness, the detectible ATP declines to 50% of its initial value in about 30 min. at 25°C. Total bleaching of the o.s. causes about a 10% fall in detectible ATP that is complete within less than 10 sec. Partial bleaching produces a smaller effect. After a bleach, the remaining ATP slowly disappears at about the same rate as before. The ATP concentration is no longer effected by light after a total bleach. Although the light-induced ATP loss is equivalent to less than 20% of the rhodopsin in outer segments, other nucleotide triphosphates are present. These may buffer the ATP level via kinases and thus the true level of PO_4 metabolism may be underestimated. ATP utilization may indeed be a direct part of the excitatory mechanism in retinal rods.

TH-PM-D3 LIGHT ENHANCES LIGHT SENSITIVITY IN CALCIUM DEPLETED RODS. S. Yoshikami† and W.A. Hagins,‡ N.I.H., Bethesda, Maryland 20014. †NEI ‡NIAMDD.

If calcium ions are internal excitatory transmitters in rod excitation, the sensitivity of the dark current to light should be affected by the amount and pKs of calcium buffers present intracellularly.

When extracellular calcium is lowered from 10^{-3}M to $<10^{-8}$M with EGTA, the light intensity necessary to suppress the dark current amplitude by 1/2 is raised from 30 to 300 hν absorbed rod^{-1} $flash^{-1}$. Rat retinas whose light sensitivity is so depressed can be restored by (a) restoring the extracellular calcium or by (b) superimposing the test flash of light on a background light, which under normal circumstances would partially suppress the dark current and thus reduce the response gain of the rods.

The drastic lowering of the extracellular calcium is thought to have its effect on the rod response (1) by decreasing Ca^{++} content and efflux from the disks in light and (2) by increasing internal Ca^{++} buffering capacity of the rod cytoplasm. Under such circumstances, the additional cytoplasmic buffer sites "Y" now compete strongly with dark current channel sites "D" for the Ca^{++} released by light from the rod disks. Consequently in Ca^{++} depleted rods, absorbed photons would be less effective in shutting down the dark current. If the "Y" sites were saturated with transmitters released by a conditioning (background) light more of the subsequent transmitter released by the test flash would be available to modulate the dark current.

TH-PM-D4 CALCIUM AND THE PHOTOTRANSDUCTION PROCESS IN THE LIMULUS PHOTORECEPTOR. M. Behbehani and R. Srebro, S.U.N.Y., Buffalo, N. Y. 14214

EGTA, a tetravalent weak acid with high affinity for Ca was injected into single ventral photoreceptors by iontophoresis. The electrode was filled with 1 M EGTA and $CaCl_2$ equilibrated to control concentrations of free Ca. Injection of EGTA equilibrated with Ca at 1.3×10^{-4} M shortened the response latency to a 10 msec light flash of low energy. At 18°C the preinjection latency, 120 msec, was reduced to 50 msec. The peak of the response was slightly increased. The effect required 1/2 hr to develop after 15' of iontophoresis at 2×10^{-9} amps. Immediately after injection the receptor was hyperpolarized and the repolarization phase of the light response was prolonged, but these effects reversed. The effect on latency was not reversible. Prolonged iontophoresis caused the light response to fail. EGTA equilibrated with free Ca at 1.5×10^{-5} M produced similar results, but the response latency was only slightly reduced, while EGTA equilibrated with 2.8×10^{-6} M free Ca slightly increased latency. Iontophoresing EGTA without added Ca caused a marked increase in response latency. Iontophoresing Cl^- had no effect at all but methylsulfate an impermeant anion, caused a transient hyperpolarization and slowing of the repolarization phase of the light response, and with prolonged injection the light response failed but there was no effect on latency. Some effects of EGTA injection are due to its being an impermeant anion, but the effects on latency are more likely due to the control of intracellular free Ca and our results can be used to estimate the normal intracellular free Ca concentration in the ventral photoreceptor is probably about 2.8×10^{-6} M. Moreover these results suggest that Ca is involved in the light induced process that leads to an increase in Na permeability.

TH-PM-D5 THE POTASSIUM DEPENDENT HYPERPOLARIZING PHOTORECEPTOR POTENTIAL: A ROLE FOR INTRACELLULAR Ca^{2+}. A.L.F. Gorman and J.S. McReynolds,*Dept. of Physiology, Boston, Mass. 02118 and Dept. of Physiology, Ann Arbor, Mich. 48104.

We have shown previously that in the distal photoreceptors of the scallop eye light activates rhodopsin which leads to an increase in K+ permeability (P_K) of its membrane and results in a hyperpolarizing receptor potential. In the dark, the photoreceptor has a low membrane potential (-33,4 mV) which is due to a high membrane permeability to Na^+ ions (P_{Na}) relative to that for K+ ions ($P_{Na}/P_K = 0.123$). The increase in P_K in light drives the membrane toward the K+ equilibrium potential ($E_K = -83.9$ mV). With maximum light intensities, the peak hyperpolarization (-74 mV) is close to E_K reflecting a sizable decrease in the permeability ratio ($P_{Na}/P_K = 0.016$). Treatment of the photoreceptor with 3 times normal external Ca^{2+} to promote a greater Ca^{2+} influx and therefore a higher intracellular Ca^{2+} concentration (Ca_i) hyperpolarizes the dark membrane potential, following a brief period of depolarization, and reduces or eliminates the photoreceptor potential. Similarly, treatment with agents, such as DNP or cyanide, which inhibit the mitochondrial uptake of free internal Ca^{2+} and therefore also increase Ca_i has the same effect. The dark membrane potential hyperpolarization is due to an increase in P_K. Conversely, inhibition of Ca^{2+} movement by the addition of 10 mM Co^{2+} or Mn^{2+} to the external medium depolarizes the dark membrane potential and produces a decrease in membrane conductance. During this period the receptor potential amplitude is decreased. We hypothesize that the light induced increase in P_K and the resulting hyperpolarizing receptor potential of these cells is mediated by an increase in Ca_2. This research supported by NIH grant EY01157.

TH-PM-D6 CALCIUM LEVELS AND LIGHT-EVOKED MEMBRANE HYPERPOLARIZATION IN APLYSIA GIANT NEURONS. F. H. Tuley*, A. M. Brown and P. S. Baur*(Intr. by F. H. Rudenberg), Department of Physiology and Biophysics, University of Texas Medical Branch, Galveston, Texas 77550.

Ca^{2+} release from cytoplasmic pigmented granules is the primary event underlying the phototransduction process in Aplysia giant neurons (Brown, Baur, Tuley, this meeting 1975). The levels of Ca^{2+} required to increase plasma membrane K^+ conductance were estimated from intracellular pressure injections of Ca EGTA buffers. A plot of the change in membrane conductance versus free Ca^{2+} contained in the injected buffers indicates a control level of 10^{-7}M. The 15% increase in membrane conductance evoked by illumination requires that free intracellular Ca^{2+} be doubled. Such small increases in free Ca^{2+} can not increase membrane K^+ conductance by screening surface charge. Assuming that the pigmented granules occupy about 1% of the cell volume, we calculate that during 15 sec. of illumination, one photon of incident light releases about 10 Ca^{2+} ions from the granules. These Ca^{2+} ions diffuse to the plasma membrane and cause about 100 K^+ ions per Ca^{2+} ion to leave the neuron. Cooling to 9°C reversibly abolishes the light response. It also appears to prevent the release of Ca^{2+} from the pigmented granules. However, cooling greatly prolongs the increased K^+ conductance elicited by intracellular Ca^{2+} injection. Conductance is restored only when the neuron is rewarmed to 18°C. Hence adaptation of the light response is not due to adaptation of the K^+ mechanism but may be related to changing levels of free intracellular Ca^{2+} during steady illumination.

TH-PM-D7 CALCIUM RELEASE FROM PIGMENTED GRANULES IS ESSENTIAL FOR PHOTOTRANSDUCTION IN APLYSIA GIANT NEURONS. A. M. Brown, P. S. Baur*, and F. H. Tuley*, Dept. of Physiology & Biophysics, Univ. of Texas Medical Branch, Galveston, Texas 77550.

Illumination of Aplysia giant neurons increases K^+ conductance of the plasma membrane (Brown & Brown, 1973). The response is simulated by intracellular pressure injection of Ca^{2+} and is reversibly blocked by injection of EGTA (Brown & Hughes, 1973). Since cytoplasmic pigmented granules show marked ultrastructural changes following illumination (Henkart, 1973) their calcium content was examined using an electron microprobe (EDAX). A pair of giant cells was dissected under red light and one neuron was exposed to white light (10^4ergs cm^{-2} sec^{-1}) for 5-30 mins. The neurons were fixed in an osmotically-buffered, 0.1M Hepes solution pH 7.4 containing 5% gluteraldehyde, post-fixed in 1% osmium tetroxide and dehydrated in ethanol. Granules from sections of 700Å thickness were examined at 20,000 magnification, 20 KeV on a Cambridge S4-10 scanning microscope and equivalent volumes from non-illuminated "dark" and illuminated "light" neurons were counted for equal periods. Compared to the spectrum for "dark" granules, the spectrum of "light" granules showed smaller peaks for Na and P and virtual absence of Ca and S peaks. These alterations in elemental composition preceded ultrastructural changes. Cooling to 9°C reversibly abolishes the light response and prevents the release of Ca^{2+} from the granules. Hence, illumination of the pigmented granules releases Ca^{2+} which diffuses to the surface membrane, increases gK and hyperpolarizes the neuron. Ca^{2+} release is the primary event in this particular phototransduction process. The mechanism in the vertebrate rod photoreceptor may be similar (Hagins, 1972).

TH-PM-D8 Ca^{++} AND H^+ DEPENDENCE, AND IONIC SELECTIVITY OF THE LIGHT-REGULATED Na^+ CHANNEL IN ROD OUTER SEGMENTS. C.M.Wormington III* and R.A.Cone, Dept. of Biophysics, Johns Hopkins University, Baltimore, Md.

We have investigated, with a variety of techniques, the osmotic responses of rod outer segments (ROS) and ROS fragments freshly isolated from the frog retina (Rana pipiens). The results reported here are based on the continuous flow technique described by Korenbrot and Cone (J. Gen. Physiol. 60,20[1972]) since this technique yields results most similar to those observed electrophysiologically in the intact retina. With the other osmotic techniques we investigated, the rate of volume recovery following a hyperosmotic NaCl shock was much slower than in the continuous flow technique, suggesting that Na permeability, P_{Na}, was greatly reduced. The cation selectivity of the light-regulated Na "channel" was determined by observing relative recovery rates following hyperosmotic shocks with Cl salts (both in light and dark). The sequence found was: $Na \approx Li >> K,Rb,Cs,Tl$ (consistent with Eisenman sequence X). The Na channel is reversibly blocked by lowering the pH; in the pH range 4.7-9.8, P_{Na} decreases with external pH with an apparent pK_a of 5.8. P_{Na} is also reduced by Ca; a marked reduction occurs when external Ca is increased from 10^{-3} to 10^{-2}M (Korenbrot and Cone). Moreover, cytoplasmic Ca appears to reduce P_{Na} much more effectively than external Ca: In the presence of the ionophore lasalocid (X537A), which presumably permits Ca to enter the cytoplasm, P_{Na} is markedly reduced when external Ca is increased from 10^{-7} to only 10^{-5}M. In a similar manner, Ca, and Ca + lasalocid, suppress the "dark-current" observed extracellularly in the isolated rat retina (Hagins and Yoshikami, Exp. Eye Res. 18,299[1974]). Our results support the hypothesis suggested by the electrophysiological results that Ca suppresses the dark-current by blocking the Na channel in the plasma membrane of the rod outer segment.

TH-PM-D9 LOCALIZATION OF A pH-SENSITIVE SITE OF METARHODOPSIN J. Lisman*, Y. Sheline*, and P.K. Brown.* (Intro. by R. Hubbard) Biological Laboratories, Harvard University, Camb., Mass. 02138

We have found that the metarhodopsin of Limulus ventral photoreceptors is an acid-base indicator whose pH-sensitive site is on the outside of the membrane. Intracellular recordings of the early potential show that at outside pH (pH_o) 7.8, light converts rhodopsin ($\lambda_{max.}$ 530 nm) to a stable photoproduct (acid metarhodopsin) with $\lambda_{max.}$ close to that of rhodopsin. At pH_o 9.6, $\lambda_{max.}$ of the photoproduct (alkaline metarhodopsin) is much shorter (below 430 nm). The effect of changing pH_o is rapid (1 min.). The following experiments suggest that these changes in $\lambda_{max.}$ depend on changes in the extracellular pH rather than on the pH inside the cell (pH_i). 1) Injection of pH 10 glycine buffer into the cytoplasm (final concentration > 100mM) does not convert acid metarhodopsin to alkaline metarhodopsin. 2) Intracellular injection of pH 7 buffer (HEPES > 100mM) does not block the effect that raising external pH has on metarhodopsin. 3) pH_i was determined by injecting the pH indicator, phenol red, into the cell and measuring its color in the microspectrophotometer. Raising pH_o from 7.8 to 9.6 causes little change in pH_i (< 0.4 pH units). Supported by NIH grants EY 00508-05 to G. Wald and EY 01496-01 to J.L.

TH-PM-D10 VISUAL FIELDS IN THE LIMULUS EYE. F.A. Dodge and E. Kaplan*; IBM Research, Yorktown Heights, N.Y. and The Rockefeller University, New York, N.Y. 10021

The dynamic response of single photoreceptors and their inhibitory interaction are well described by the (time-dependent) Hartline-Ratliff equations. To compute how a pattern of illumination in space is mapped into the pattern of optic nerve activity we must also know (1) how the ommatidial optics sample visual space and (2) the spatial dependence of inhibition converging onto an ommatidium. Taking advantage of the remarkable linearity of the response of this retina to incremental stimuli, we measured modulation to the spike rate of an ommatidium which looked at a TV-like display where the intensity of a thin bar was sinusoidally modulated around the same mean intensity as the background. Responses measured at different bar positions map the visual field which has an excitatory center and inhibitory surround. The central field is gaussian about 7^o wide at half height (range 4^o (extreme light adaptation) to 10^o). In a horizontal plane the directions of the optic axes of adjacent ommatidia diverge uniformly by about 4.5^o, and the inhibitory field is broad and flat. In a vertical plane, divergence is not uniform, being over 7^o above, and less than 2.5^o below, the center, and the inhibitory fields are generally asymmetrical. We have compared the measured inhibitory fields with solutions of a Hartline-Ratliff model that take explicit account of the orientation of optical axes. From these computations we conclude, in agreement with previous work, that the map of retinal connectivity is center-symmetric with eliptical contours, but it is flatter and broader than that deduced from measurement of single unit interactions. This research was supported in part by Grants EY188 and NSF-GB36168, and Fellowship EY3220, to E. Kaplan.

TH-PM-D11 THEORY OF SUSTAINED OSCILLATIONS IN THE RESPONSE OF THE LIMULUS RETINA TO UNIFORM EXCITATION. B. D. Coleman*, Departments of Mathematics and Biology, Carnegie-Mellon University, Pittsburgh, Pa. 15213, and G. H. Renninger, Department of Physics, University of Guelph, Guelph, Ontario N1G 2W1.

Existing experimental observations indicate that, for the compound eye of Limulus, the response to a spatially uniform excitation e (in the usual Hartline-Ratliff units) should be a solution of the equation

$$r(t) = m\left(e(t) - \frac{A}{\delta}\int_0^\infty e^{-s/\delta} r(t-\tau-s)ds\right), \qquad (1)$$

with m the "positive part" function defined by $m(x) = \frac{1}{2}(x+|x|)$. Here A, τ, and δ are positive constants: A/δ measures the rate at which lateral inhibition is increased by response; τ is the delay in such increase; and δ is the relaxation-time for the decay of inhibition. We show that if A and τ/δ are in appropriate ranges, then, for e held constant, (1) has a non-constant periodic solution which can be written in closed form in terms of elementary functions. This solution shows a sustained synchronous "bursting phenomenon" in which the time-intervals of neural activity in the optic nerve alternate with rest periods. When A is sufficiently small, the function m does not affect solutions of (1), and (1) can be solved analytically even for time-varying e; solutions obtained for small A exhibit transient rather than sustained oscillations.

TH-PM-D12 REPEATED GROUPINGS OF CONE TYPES IN THE TURTLE'S RETINA. L.E. Lipetz, Dept. of Biophysics, The Ohio State Univ.,Columbus,Ohio 43210.

The pigment epithelium was removed from freshly excised retinas of the turtle, Pseudemys scripta elegans, which were then laid flat and photomicrographed from the visual cell side. The resulting color slides were projected, the outlines of the visual cells traced and labeled as to presence or absence of oil droplet and its color. Six types of visual cell were identified: single cones with clear (C), yellow (Y), or red droplet (R); a double cone consisting of a chief cone with an orange droplet (O) and an accessory cone with no droplet; a few single rods with no droplet. The total cone density and the ratios of cone types were determined for many retinal regions. High (H) densities were found in the horizontal streak region, medium (M) nearby, and low (L) farther from the streak. The cone type ratios differed for H vs L, with M ratios intermediate. The ratio of R to total varied from region to region even for the same densities. If only O, Y and C cones were considered, their ratios were the same from L region to L region for the same and different (3) retinas,being close to 3(C) to 4(Y) to 5(O). This suggests that these cone types form a group (or groups totalling to that ratio) which are repeated throughout the L areas.

A preliminary analysis of the local geometry of cone distributions was done in terms of their positions and distance around each cone of a given type. A grouping with 50% greater occurrence than expected from overall cone ratios was found to lie in a straight line. It was C-2-O-1-C-1-O, where the 1 or 2 gives the number of intervening 20μm distances. A grouping with 30% greater occurrence was O-2-C-2-O, with the O-C-O in a straight line (at 90° to the above C-O-C-O line) $\diagdown^{2}$ and the C-(CY) line at 45° to it. These may be the visual cell $\diagdown_{(CY)}$ groupings underlying some of the feature extraction properties of the turtle's retina.

TH-PM-D13 TUNABLE LASER RESONANCE RAMAN SPECTROSCOPY AS A PROBE OF PRIMARY ION MOVEMENTS IN PHOTORECEPTOR CELLS. Aaron Lewis, School of Applied and Engineering Physics, Cornell University, Ithaca, New York 14853.

We have demonstrated[1] using resonance Raman spectroscopy that the Schiff base linkage in bovine and bacteriorhodopsin is protonated. In addition we have recently shown that a result of the transduction of light energy into chemical energy by rhodopsin involves the release of the Schiff base proton between the Meta I and Meta II thermal intermediates of rhodopsin. The neural impulse is generated on the same time scale as the release of the Schiff base proton and overall proton release and uptake by rhodopsin also occurs on a similar time scale. A principal experimental difficulty we encountered in obtaining Raman spectra of rhodopsin was fluorescence. We narrowed down the fluorescence problems to the pigments in the pigment epithelium and when we separated these pigments from the retina we obtained retinal preparations that gave exceptional Raman spectra. However, albinos naturally select against these fluorescing pigments, and therefore we used a New Zealand white rabbit to obtain the resonance Raman spectrum of the retinylidene chromophore of rhodopsin in an intact eye. We extended these measurements to obtain similar Raman spectra in a live eye while simultaneously monitoring and stimulating an electroretinogram with a variable intensity 500nm light source. Changes in the vibrational spectrum of the retinylidene chromophore were observed when a neural impulse was generated by the photoreceptor cell. In vitro modeling experiments indicate that our in vivo Raman spectra of rhodopsin can act as an effective probe of the primary ion movements associated with visual response.

1. A. Lewis et al., J. Raman Spectrosc. 1, 465 (1973); A. Lewis et al., in Neutron, X-Ray and Laser Spectroscopy in Biophysics and Chemistry, S. Chen and S. Yip eds. (Academic Press, New York, 1974), p. 347.

TH-PM-E1 CIRCADIAN CLOCK MODULATION OF THE CELL DEVELOPMENTAL CYCLE IN MUTANTS OF EUGLENA: COUPLING EFFECTS OF SULFUR-CONTAINING COMPOUNDS.

L. N. Edmunds, Jr.*, M. E. Jay*, A. Kohlmann*, S. C. Liu*, and H. Sternberg* (Intr. by Elkan Blout), Department of Cellular & Comparative Biology, State University of New York at Stony Brook, Stony Brook, New York 11794.

Previous work has demonstrated a persisting, freerunning, circadian rhythm of cell division in the P_4ZUL photosynthetic mutant of the alga Euglena gracilis Klebs (Strain Z) Pringsheim grown organotrophically in continuous light or darkness at 19°C following prior synchronization by a repetitive LD: 10,14 cycle [Jarrett, R. M. and L. N. Edmunds, Jr., Science, 167: 1730-1733 (1970)]. A similar circadian rhythmicity has been recently discovered in the W_6ZHL heat-bleached mutant of Euglena grown under comparable conditions. Over extended timespans, however, these mutants appear to gradually lose first their ability to display persisting overt rhythms, and then even their capability of being entrained by imposed LD cycles. Interestingly, these properties can be restored by the addition of certain sulfur-containing compounds to the medium. These include cysteine, methionine, dithiothreital, Na_2S, $Na_2S_2O_3$, and possibly Na_2SO_3. The implications of these findings towards biological clock mechanisms are discussed.

TH-PM-E2 NEURONAL CIRCADIAN OSCILLATORS IN APLYSIA: POPULATIONS VS SINGLE NEURON. Jon W. Jacklet and Christine Lukowiak*, Department of Biological Sciences, State University of New York at Albany, Albany, N.Y., 12222.

Several neuronal structures in Aplysia have been rigorously tested for the characteristics of a circadian rhythm in neuronal activity. One of these, the eye, is a circadian oscillator since it has a regular, predictable waveform with a period of 26-27 hours that persists for 2 weeks in constant in vitro conditions. A single neuron, the parabolic burster described by Strumwasser (1965) as a circadian oscillator, has an irregular, unpredictable waveform which is not periodic when maintained for a week in constant in vitro conditions. The first peak in activity, that led to the earlier speculation that it was a circadian oscillator, is reproducible and predictable by considering both the light-dark history of the animal and the time of dissection (Lukowiak, 1974). This cell is quite sensitive to 24 hour cycles of temperature and synaptic input, and is thus an excellent follower, but the driven activity will not free-run when it is released into constant conditions. Presently, no single neuron has been demonstrated to be a circadian oscillator. The precision of the eye circadian rhythm is apparently attributable to a population of coupled neurons. Experimental reduction of the number of neurons in the eye influences both the amplitude and the period of the oscillations. Electrical recording and dye marking of neurons shows that the major retinal neurons have axons in the optic nerve and there is no unique neuron but rather a population of electrotonically coupled neurons.

TH-PM-E3 RHYTHMIC CHANGES IN K+ CONTENT AND ELECTRICAL PROPERTIES OF PLANT MOTOR CELLS. R.L. Satter* and A.W. Galston*, Biology Dept., Yale University New Haven, Conn. 06520 and Richard Racusen*, Botany Dept., University of Vermont, Burlington, Vermont 05401. (Intr. by D. Branton)

Rhythmic and light-regulated leaflet movement in Albizzia and Samanea are controlled by changes in the relative turgor of flexor and extensor motor cells located on opposite sides of the pulvinus. Turgor in turn is regulated by K+ content, as determined by electron microprobe measurements. Increase in K+ in the extensor cells and decrease in K+ in the flexor cells lead to opening while K+ fluxes in the reverse directions lead to closure. Inhibitors of oxidative phosphorylation as well as low temperature impede rhythmic opening but promote rhythmic closure, suggesting that the rhythm involves the alternating predominance of ion pumps and leakage through diffusion channels, each stage lasting ca. twelve hours. Impalement of motor cells with microelectrodes revealed circadian oscillations in potential in both extensor and flexor cells. The flexor cells hyperpolarize during the energy-requiring period of the rhythm and depolarize during the leaky period; the extensor cells start depolarizing 6 hours earlier. Light affects the rhythm via two photosystems: 1) Prolonged irradiation with high intensity blue light promotes K+ secretion from the flexor cells and leaflet opening. 2) Brief irradiation with red and far-red light absorbed by the membrane-localized chromoprotein phytochrome regulate K+ flux and leaflet movement during dark-induced closure and during the energetic portion of the rhythm. Both photosystems affect membrane potential within 15-90 seconds after the onset of irradiation; these changes precede K+ flux and leaflet movement. Combined evidence suggests the membrane as a common locale for the action of all three regulatory systems.

TH-PM-E4 HOLDING THE GONYAULAX CLOCK AT A UNIQUE PHASE POINT WITH BRIGHT LIGHT OR LOW TEMPERATURE: IMPLICATIONS FOR A MEMBRANE CLOCK MODEL. David Njus and J.W. Hastings, Harvard University, Cambridge, MA 02138.

Both bright light (greater than 1000 fc) and low temperatures (less than 13°) cause the Gonyaulax clock to settle into a unique phase point. When cells are removed from these conditions, the circadian rhythm resumes with a phase determined by the time of removal. The clock appears to hold at CT 12, the phase corresponding to the end of the light period in a 12:12 light:dark cycle. A membrane model for the circadian clock (Njus et al., Nature 248, 116, 1974) proposes that light shifts the phase of the clock by changing ion concentration gradients across a membrane. Bright light acts by driving the ion gradient to a unique level (probably equilibrium). Low temperature should also act this way, presumably by opening ion-conducting channels in the membrane. The holding effect occurs at 12.5° but not at 14° indicating that the cut-off is very well-defined. This correlates with another effect attributable to temperature-dependent permeability changes; bioluminescence is stimulated when the temperature drops below 13°, apparently because of an effect on an excitable membrane controlling luminescence. Since K+ ions are implicated in the clock mechanism, an attempt was made to alter the unique phase point achieved at low temperatures by changing the K+ concentration of the growth medium. This should change the K+ equilibrium across the cell's external membrane and consequently alter any equilibrium attained at low temperatures. This treatment did not affect the unique phase point suggesting that 1) K+ is not the ion involved in the clock, 2) the phase shifting mechanism proposed is incorrect, or 3) the membranes involved in the clock are internal. Reasons for favoring the final possibility will be discussed. Supported by NIH grant GM 19536.

TH-PM-E5 DROSOPHILA'S CLOCK PHOTORECEPTOR IS STILL NOT RHODOPSIN. A. T. Winfree, Dept. Biol. Sci., Purdue University, W. Lafayette, Ind. (Intr. by Jerome Schiff)

A circadian rhythm governs the eclosion time of Drosophila pupae. Though its phase can be reset by as little as 100 ergs/cm^2 of blue light (460 nm.) it is 10-100 times less sensitive during the first 30 hours after prolonged illumination. Exposure to at least 2x10^7 ergs/cm^2 reverses this dark-adaptation(1). This fact, the action spectrum for rephasing(2), and the rhythm's normal photosensitivity in visually deficient flies deprived of carotenoids(3) argue that the clock's photoreceptor is not rhodopsin. But doubt was raised by the recent discovery(4) of a photoreversible transition in Drosophila rhodopsin between the blue-absorbing form and a relatively stable orange-absorbing form. In these experiments consistent absorption levels were found only after at least 24 hours' dark-adaptation. Could the clock's peculiarly slow dark adaptation reflect the slow thermal reversion of insect rhodopsin from orange-absorbing to blue-absorbing states? In short, I think not. Using the 589 nm sodium doublet at energies up to 2x10^7 ergs/cm^2 in an extensive series of experiments, we were unable to demonstrate any effect either directly on the rhythm's phase or on its photoreceptor's sensitivity toward blue light. Thus rhodopsin remains an unlikely candidate for the clock photoreceptor in Drosophila pupae. I thank S. Ostroy for bringing his discovery to my attention and suggesting these experiments, Herman Gordon for doing the work, the NSF for research support and the NIH for a Research Career Development Award.

1) Winfree, A.T. J. Theor. Biol. 35, 159 (1972)
2) Zimmerman, W.F. and D. Ives in Biochronometry, ed. M. Menaker (1971).
3) Zimmerman, W.F. and T.H. Goldsmith, Science 171,1167-1169 (1971).
4) Ostroy, S.E., M. Wilson, and W.L. Park, B.B.R.C. 59, 960-966 (1974).

TH-PM-E6 A GENERAL METHOD FOR DISTINGUISHING THE FUNDAMENTAL TIMER FOR A BIOLOGICAL RHYTHM FROM CYCLIC PROCESSES WHICH IT TIMES. L. J. Mets*, (Intr. by M. Schoenberg), National Institutes of Health, Bethesda, Maryland 20014.

Variability of intervals between successive events in biological rhythms is an important consequence of the particular mechanism which generates the rhythm. Analysis of this variability has not previously been exploited as a tool for investigating the nature of these rhythms. This is done by establishing synchrony among a population of individuals (either analytically or experimentally) and then by following the desynchronization under constant conditions. A variance function is obtained by plotting the population variance of the times of occurrence of events in the 1st, 2nd, ..., nth post synchrony cycles versus the cycle number. When this plot yields a straight line, its slope is a measure of the variance of the fundamental timer for the rhythm. Its intercept is related to the variance of the cued output process. The interpretation of other shapes of the variance function depends upon the exact experimental protocol. The development of these techniques for analyzing human fingertapping rhythms will be illustrated. Analysis of literature data from circadian rhythms in Drosophila indicate that although the period of the circadian clock is insensitive to temperature, its precision is temperature dependent, as are properties of the coupling of the clock to the observed events. Persistent synchrony of cell division in Euglena populations can be explained without requiring intercellular communication and mutual synchronization. A general procedure for obtaining maximum information from short term studies of circadian rhythms will be discussed.

Biophysical Journal vol. 15, 1975 178a

TH-PM-E7 PACEMAKER BEHAVIOR IN ENTRAINED FIREFLY FLASHING. J. Buck,* J. Case,* F. Hanson,* and E. Buck* (Intr. by E. Kempner), National Institutes of Health, Bethesda, Maryland 20014, Department of Biological Sciences, University of California, Santa Barbara, California 93106, and Department of Biology, University of Maryland, Catonsville, Maryland 21228.

Several New Guinean species of firefly habitually flash in rhythmic synchronism with a period of about 1000 msec. Artificial driving of individuals showed ability to engage in steady state anticipatory entrainment at periods ranging from 800 to 1800 msec, with the change from free run period being nearly proportional to phase of driver signal entry. Free run flashing statistics, phase-shifting transients and responses to overlong and overshort drivers and to random challenges were all consistent with an entrainment mechanism in which light resets the endogenous pacemaker in an all-or-none and cycle-by-cycle fashion. Tentative analogies with pacemaker neuron behavior will be pointed out. We acknowledge the support of the National Science Foundation for our Alpha Helix Expedition.

TH-PM-E8 CIRCADIAN ACTIVITY OF A NICKEL COATED GLASS SLIDE USED FOR CARRYING OUT IMMUNOLOGIC REACTIONS AT A LIQUID-SOLID INTERFACE. Alexandre Rothen, The Rockefeller University, New York, N.Y. 10021.

Active nickel plated glass slides are prepared by evaporating the metal *in vacuo* in the presence of a magnetic field oriented perpendicularly to the slide, the surface being metallized facing the south pole of the field. Inactive nickel plated slides are obtained by carrying out the evaporation in the absence of a magnetic field. Active slides coated with an antigen layer (serum bovine albumin or ovalbumin) can specifically adsorb a layer of antibodies nearly twice as thick (70 to 80 A) as that adsorbed on inactive slides (40 A) provided the serum is diluted at least 1/100. The activity of a slide varies with an exact 24-hour period. Fully active at night, a slide gradually loses its activity after sunrise and has recovered it at sunset. Activation and inactivation can be prevented by shielding the slide with 3.5 cm of lead. The experimental evidence favors the view that inactivation is brought about by soft cosmic rays from the sun.

TH-PM-E9 PARTIAL PEELING IN BIOLOGICAL OSCILLATIONS, Okan GUREL, IBM Corporation Scientific Centers, White Plains, New York 10604.

In spite of recent advances made in modelling biological oscillators, biological oscillations both in neurobiological [O. Gurel, Biophysics Society 18th Meeting Abstracts, Minneapolis, Minnesota (1974)] and biochemical systems [O. Gurel, FEBS 9th Meeting, Budapest, Hungary (1974)] are still in their infancy. The reason for this is the limitation in the mathematical theory and in the knowledge of biophysicists and biochemists. Here, two models due to O. Rossler are discussed, both leading to partial peeling [O. Gurel, Int. Symposium in Dynamical Systems, Brown University, Providence, R. I. (1974)] in which limit cycles are obtained surrounding a saddle point contrary to those well-kown limit cycles surrounding singular points of the types node or focus. Examples involve three or six dimensions and a number of parameters, some of which are peeling parameters.

TH-PM-E10 OSCILLATIONS IN NEGATIVE FEEDBACK CELLULAR CONTROL SYSTEMS. S. Hastings* and J. Tyson* (Intr. by F. Snell), Department of Mathematics, State University of New York at Buffalo, Buffalo, New York 14221.

Feedback inhibition in a sequence of biochemical conversions

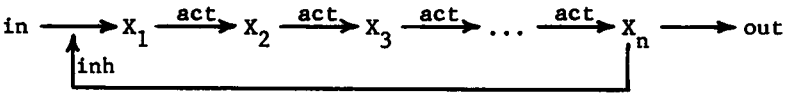

often produces sustained (limit cycle) oscillations. The extensive digital calculations carried out by Walter suggest the existence of limit cycles whenever the steady state behavior is unstable with respect to small perturbations. The existence of a periodic solution for this scheme whenever the steady state solution is unstable is established rigorously by an extension of the Poincaré-Bendixson Theorem. Walter's calculations also suggest that when the steady state is stable with respect to small perturbations, it is also stable with respect to arbitrarily large perturbations. However, investigation of this case by Hopf's bifurcation theory casts doubt on this latter claim.

Biophysical Journal vol. 15, 1975 **180a**

TH-PM-E11 TIME DELAY, EPIGENETIC DYNAMICS, AND CIRCADIAN OSCILLATIONS. Andrew G. De Rocco and John Avitabile, Institute for Molecular Physics, University of Maryland, College Park, Maryland, 20742.

The Goodwin equations representing epigenetic dynamics are modified by introduction of a time delay intended to represent the lag between transcription and translation; other events are taken as spatially and temporally uniform. For a suitably 'large' (non-zero) value of the time delay the system of coupled equations representing mRNA and enzyme synthesis achieves a self-sustained limit cycle. If departures from a stability locus are linearized, a condition on the time delay can be found which just insures oscillatory behavior. For a cycle time of 24 hours the required delay is ca. 24', a figure in general agreement with published figures for the time delay in mRNA transport across the nuclear envelope. We argue that the constants appropriate for the Goodwin equations should be those 'renormalized' to include intercistronic interactions, for it is from such a coupled system that a circadian oscillation can emerge.

TH-PM-E12 NONLINEAR WAVES IN CHEMICALLY-REACTING SYSTEMS. H. G. Othmer, Department of Mathematics, Rutgers University, New Brunswick, NJ 08903.

It has frequently been suggested that propagating chemical waves can serve as a means of communication and control in developing biological systems. We consider reacting systems governed by the equation $\frac{\partial c}{\partial t} + f(c)\frac{\partial c}{\partial x} = D\frac{\partial^2 c}{\partial x^2} + R(c)$ where c is chemical concentration, $f(c)\frac{\partial c}{\partial x}$ describes active or convective transport, $D\frac{\partial^2 c}{\partial x^2}$ diffusive transport, and $R(c)$ chemical reaction and exchange. Under appropriate restrictions on $f(c)$ and $R(c)$, the equation is similar to those arising in models of nerve impulse conduction. When $f(c) \equiv 0$, it is known that change of state waves exist for a certain class of functions $R(c)$. We show that when $f(c) \not\equiv 0$, both periodic and solitary (pulse) waves also exist for a large class of functions $f(c)$. The stability of these waves and their relevance to communication in biological systems will be discussed.

TH-PM-F1 THE BINDING OF NADH TO GLUTAMATE DEHYDROGENASE. Barbara D. Wells, Institute of Molecular Biophysics, Florida State University, Tallahassee, Florida 32306.

The circular dichroism (CD) between 350 and 200 nm has been measured for glutamate dehydrogenase alone and with NADH. The spectral region measured covers both the coenzyme chromophore bands as well as the protein backbone. Previously CD data has been cited as direct evidence for a second NADH binding site (Krause, et al., Eur. J. Biochem. 41, 593 (1974)). However, it has been found in studies to be reported here that the CD band implicated in this second site interpretation is dependent upon protein concentration and not simply the ratio of coenzyme to enzyme. Therefore the CD spectral evidence for a second binding site is complicated by protein aggregation. Since the pertinent kinetic data were obtained at low enzyme concentrations, additional CD and kinetic data must be taken at comparable enzyme concentrations before a definitive interpretation is possible. (Supported by USPHS Grant GM-17506 to J. R. Fisher and by the Division of Biology and Medicine, AEC.)

TH-PM-F2 COENZYME BINDING BY NATIVE AND CHEMICALLY MODIFIED PIG HEART TPN-DEPENDENT ISOCITRATE DEHYDROGENASE. Robert Ehrlich* and Roberta F. Colman* (Intr. by Dr. N. Ramachandran.) Department of Chemistry, University of Delaware, Newark, Delaware, 19711.

To characterize the effects of chemical modification of TPN-specific isocitrate dehydrogenase, coenzyme binding was measured by the techniques of fluorescence enhancement and ultrafiltration. A single TPNH binding site is observed with a dissociation constant of 1.5 uM. Manganous ion does not change the binding of free TPNH and isocitrate alone has only a weak effect on TPNH binding. In contrast, competition for the TPNH site by the true substrate manganous-isocitrate complex (K_I = 1.6 uM), as well as the reciprocal competition of TPNH for the binding of Mn-isocitrate, suggests that the substrate and reduced coenzyme occupy mutually exclusive or overlapping sites on the enzyme. TPN also competes with TPNH. TPN binds weakly to two sites with a dissociation constant (K_D = 50 uM) an order of magnitude greater than its K_m. When isocitrate is added, the binding to one site is markedly enhanced (K_D = 0.6 uM). These results imply that TPN is not the initial component to bind to the enzyme in the forward reaction. Enzyme inactivated by reaction of glycinamide with a glutamate, of cyanide with four cysteines and of N-ethyl maleimide with two cysteines fails to bind either TPNH or manganous-isocitrate, supporting the close relationship between these sites observed for native enzyme. In contrast, inactive enzyme prepared by reaction of iodoacetate with a methionine is able to bind manganous-isocitrate but not coenzyme; in this case, disruption of the coenzyme binding site may be chiefly responsible for the inactivation. (Supported by N.I.H. Grant AM-17552.)

TH-PM-F3 THE TWO-STAGE REVERSIBLE DISSOCIATION OF LACTATE DEHYDROGENASE AT LOW pH. R.B. Vallee and R.C. Williams, Jr., Department of Biology, Yale University, New Haven, Connecticut 06520.

Beef B_4 lactate dehydrogenase is inactivated within 15 seconds at 0° in 0.1 M sodium phosphate buffer, pH 2-3. It has been shown that full and rapid reactivation following second-order kinetics can be achieved if the enzyme is returned to neutral pH within 30 seconds of exposure to pH 3.0 (Anderson, S. and Weber, G., Arch. Biochem. Biophys. 116: 207, 1966). Longer exposure results in a loss of recoverable activity. We find that recoverable activity declines to a value of 50-60% within 10 minutes at pH 3.0, but then becomes nearly constant, showing further decline at a rate of only 10% per day. The overall time-course of reactivation for enzyme exposed to acidic conditions for longer than 10 minutes is independent of protein concentration, occurring with a half-time of 15 minutes at 20°. The change in the kinetics of reactivation with time of exposure to low pH suggests that the enzyme passes through an intermediate dissociated state before reaching a relatively stable denatured form. Two fractions are obtained from denatured protein chromatographed on Sephadex G-100 at pH 2 or 3. The lower molecular weight fraction is capable of recovering enzymatic activity, and , as indicated by equilibrium ultracentrifugation, is in the form of fully dissociated subunits. The higher molecular weight fraction, which shows no recovery of activity, is generated from the lower molecular weight material and may become predominant under conditions of increased pH, temperature, and protein concentration. The results suggest a mechanism for the denaturation of lactate dehydrogenase in which dissociation of the native tetramer is followed by a second, kinetically distinguishable step leading to conformationally disorganized subunits.

TH-PM-F4 INCREASED ENZYMATIC ACTIVITY FOR NANOMOLAR CONCENTRATIONS OF HORSE LIVER ALCOHOL DEHYDROGENASE. Barbara F. Howell. NBS, Washington, D.C. 20234

Rate measurements for the reaction between reduced nicotinamide adenine dinucleotide (NADH) and acetaldehyde in the presence of horse liver alcohol dehydrogenase were made at enzyme concentrations ranging from 0.15 to 10 nmol/l. Repeated trials gave the result that, at concentrations lower than 1.6 nmol/l, ratios of the reaction velocity to the enzyme concentration increase markedly. This rate increase may be attributed to dissociation of the dimeric enzyme into monomeric units which are enzymatically more active than is the dimer. By use of equations developed by Kurganov [Molkulyarnaya Biologiya 2 (No. 2), 166 (1968)] we arrive at the value $4.0 \pm 0.9 \times 10^9$ 1/mol for the monomer to dimer equilibrium constant at 25°C.

TH-PM-F5 CIRCULAR DICHROISM STUDIES ON DIHYDROFOLATE REDUCTASE FROM METHOTREXATE-RESISTANT SARCOMA 180 CELLS. Myra N. Williams, Merck Institute for Therapeutic Research, Rahway, N.J. 07065.

The circular dichroism of Sarcoma 180 (S-180) dihydrofolate reductase is quite different from that of *E. coli* dihydrofolate reductase. The S-180 enzyme exhibits a molar ellipticity approximately 3-fold greater than that of the *E. coli* enzyme (Greenfield *et al*, *BIOCHEMISTRY 11*, 4706, 1972). Since the S-180 enzyme is activated by NaCl, the circular dichroism was measured from 190 to 400 nm at varying ionic strengths to probe for conformational changes. While there are small differences in the aromatic region of the activated enzyme as compared to the unactivated form, there are no detectable changes in the peptide backbone region. The binding of either dihydrofolate or TPNH to the enzyme induces large extrinsic cotton effects and the binding of TPNH causes slight changes in the peptide backbone region. The homologies of the circular dichroism spectra of the S-180 and *E. coli* enzyme-dihydrofolate complexes suggest that the conformation of bound dihydrofolate in the active sites is quite similar. The same conclusion can be drawn for the respective enzyme-methotrexate-TPNH complexes.

TH-PM-F6 DIHYDROFOLATE REDUCTASE FROM A METHOTREXATE-RESISTANT *ESCHERICHIA COLI:* CONTRIBUTION OF IONIC BONDING TO INTERACTION WITH 5- AND 6-SUBSTITUTED QUINAZOLINES AND 6- AND 7-SUBSTITUTED PTERIDINES. Martin Poe, Merck Institute for Therapeutic Research, Rahway, New Jersey 07065.

The inhibitory constants K_i and acid dissociation constants pKa have been determined for eleven sterically similar inhibitors of *E. coli* MB1428 dihydrofolate reductase that are competitive inhibitors of the substrate dihydrofolate. These compounds are 5- and 6-substituted 2,4-diamino-quinazolines and 6- and 7-substituted 2,4-diamino pteridines. A sigmoidal relationship was found between the K_i and pKa values for this series of inhibitors and explained by an ionic bonding hypothesis. In this hypothesis, the neutral and protonated forms of these inhibitors have vastly different inhibitory potencies, with $K_i = 1.35 \times 10^{-4}$ M and 1.45×10^{-9} M, respectively, for the series of inhibitors reported here. A schematic molecular model for the hypothesis will be presented. In this model a proximal ionized carboxyl moiety of the protein increases the proton affinity of enzyme-bound inhibitors. The resulting salt linkage of proximal negatively charged carboxyl moiety and positively charged inhibitor is responsible for the tighter binding of the positively charged form of the inhibitor. At neutral pH 2,4-diamino compounds exhibit a much higher proportion of positively charged inhibitor than the corresponding 2-amino-4-hydroxy compounds, i.e. their pKa values are 3 to 4 units higher and they are thus better inhibitors. These results appear to confirm the ionic bonding hypothesis as explaining the difference in binding of folate and methotrexate by *E. coli* MB 1428 dihydrofolate reductase, and provide a plausible explanation for the changes in the ultraviolet absorbance noted upon binding of methotrexate to the enzyme.

TH-PM-F7 CALCULATION OF BASE AND E. COLI DIHYDROFOLATE REDUCTASE INHIBITORY STRENGTHS FOR A SERIES OF STERICALLY SIMILAR PTERIDINES AND QUINAZOLINES. David D. Saperstein*, Merck Sharp & Dohme Research Laboratories, Rahway, N. J. 07065 Introduced by Karst Hoogsteen.

This work demonstrates that the basicities estimated using calculated charge densities and coulomb integrals obtained in the CNDO/2 method correlate strongly with both the pK_a [cation dissociation constant] and pK_i [dihydrofolate reductase (DHFR) inhibition constant] for a series of sterically similar inhibitors of DHFR extracted from methotrexate resistant E. coli (MB 1428). Specifically, the basicity estimated at the N_1 position for 6,7-substituted (Cl, NH_2, etc) 2,4-diaminopteridines and 5,6-substituted 2,4-diaminoquinazolines correlates to a very significant level ($P < 0.001$), whereas the basicity estimated at other positions (N_3, etc) do not correlate well with pK_a or pK_i. This specific correlation is consistent with the ionic binding hypothesis for these inhibitors to DHFR through an amidinium ion formed at the N_1-2-amino portion of the inhibitor.

TH-PM-F8 ANALYSIS OF THE ALLOSTERIC BASIS FOR POSITIVE AND NEGATIVE COOPERATIVITY AND HALF-OF-THE-SITES REACTIVITY IN YEAST AND RABBIT-MUSCLE GLYCERALDEHYDE-3-PHOSPHATE DEHYDROGENASE. J. Herzfeld and P.A. Schlesinger* Department of Chemistry, Amherst College, Amherst, Maasachusetts 01002.

A general model of cooperativity has been used to analyze equilibrium dialysis and thermal titration measurements of NAD binding, and measurements of the NAD dependence of proteolytic inactivation and enzyme activity. The results suggest that glyceraldehyde-3-phosphate dehydrogenase (GPDH) has two quaternary conformations and that the change from the quaternary conformation of the apoenzyme to that of the holoenzyme occurs roughly when the first NAD molecule binds; this change is responsible for the fact that in yeast GPDH the second NAD molecule has a higher binding affinity than the first, and that the resistance of yeast and rabbit-muscle GPDH to proteolysis increases sharply when the first one or two NAD molecules bind. In addition, within the quaternary conformation of the holoenzyme, NAD binding at different sites is coupled by a tetrahedral (rather than square or dimer) pattern of antagonistic interactions; these interactions are responsible for negative cooperativity in GPDH. Since little or no NAD can be bound to the enzyme when it is in the quaternary conformation characteristic of the apoenzyme, this quaternary conformation is found to be essentially inactive. Half-of-the-sites reactivity can be explained by supposing that modification of the cysteine-149 sulfhydryl groups stabilizes the inactive quaternary conformation of the enzyme. In contrast to other proposed explanations of half-of-the-sites reactivity, this explanation does not assume molecular asymmetry or direct interactions between sites, and is therefore also applicable to enzymes which show no negative cooperativity.

TH-PM-F9 ENZYME·PRODUCT DISSOCIATION AS THE RATE-LIMITING STEP IN THE SYNTHESIS OF AMINOACYL-tRNA? R.B. Loftfield and T.N.E. Lövgren. University of New Mexico, School of Medicine, Albuquerque, NM 87131

These events are proposed for aminoacylation of tRNA (Biochem. 11, 17):

$$\text{Enz} + \text{ATP} + \text{AA} \longrightarrow \text{Enz}\cdot(\text{AA}\sim\text{AMP}) + \text{PP}_i \qquad k > 10^{-1}\ \text{sec}^{-1}$$

$$\text{Enz}\cdot(\text{AA}\sim\text{AMP}) + \text{tRNA} \underset{k_2}{\overset{k_1}{\rightleftharpoons}} \text{Enz}\cdot(\text{AA}\quad\text{AMP})\cdot\text{tRNA}$$

$$\text{Enz}\cdot(\text{AA}\sim\text{AMP})\cdot\text{tRNA} \xrightarrow{k_3} \text{Enz}\cdot(\text{AA-tRNA}) + \text{AMP} \qquad k_3 \cong .02\ \text{sec}^{-1}$$

$$\text{Enz}\cdot(\text{AA-tRNA}) \xrightarrow{k_4} \text{Enz} + \text{AA-tRNA} \qquad k_4 \cong .002\ \text{sec}^{-1}$$

We find that, under experimental conditions similar to those used in developing the above scheme, the overall reaction is strongly inhibited by salt. When the log (rate) is plotted against $\sqrt{\mu}/(1 + \sqrt{\mu})$ the Debye-Hückel coefficient is -11 indicating a rate limiting step of association between multiply ionized molecules of opposite charge. k_3 is relatively insensitive to ionic strength. k_4, as measured by the Yarus assay (JMB 42, 171), increases rapidly with μ, the Debye-Hückel coefficient being +6. For the above sequence of reactions, the overall rate, v, is

$$v = \frac{k_3[E_o]}{(k_2 + k_3)/k_1 + [\text{tRNA}](1 + k_3/k_4)} \text{ and } V_{max} = \frac{k_3k_4[E_o]}{k_3 + k_4}.$$ Conditions

that increase k_4 must increase V_{max} almost in proportion regardless of the effect on k_3. Only if $k_4 \gg k_3$ can V_{max} be insensitive to changes in k_4, a conditional inconsistent with dissociation being rate-limiting. We conclude that rate or extent of association of tRNA with enzyme is rate-limiting. USPH CA-08000 Am. Cancer Soc. NP104.

TH-PM-F10 CONDENSED PEROXIDASE REACTION KINETICS UNDER LOW-WATER ACTIVITY. Chattopadhyay, S.K. and Brown, H.D., Rutgers University, New Brunswick, New Jersey, U.S.A.

"Macrocrystals" of peroxidase (E.C.1.11.1.7) have been prepared by condensation using N-N'-carbonyldiimazole as the activating agent. Catalytic synthesis of 2,6 dimethylbenzoquinone-4-(2',4'-6'-trimethyl) anil from mesidine has been studied in binary ethanol-water mixtures containing 1, 5, 10, 20 and 50 percent ethanol. The stabilized macrocrystals (M.S. > 150,000) were active in binary mixture environments and the reaction kinetics were a function of the nature of the condensed enzyme and of the concentration of organic solvent in the mixture. Supported by National Science Foundation.

TH-PM-F11 NOISE AND FLUCTUATIONS IN LINEAR KINETIC SYSTEMS AT CYCLING STEADY STATE. Yi-der Chen, Laboratory of Molecular Biology, NIAMDD, National Institutes of Health, Bethesda, Md 20014

Cyclic biochemical reactions are very common in biological systems. Recently, a linear model with cyclic splitting of ATP (or GTP) and cyclic protein conformational transformation has been proposed to explain the mechanism of active transport, muscle contraction, protein synthesis, etc. (T. L. Hill, Proc. Natl. Acad. Sci. 64, 267 (1969)). In biochemistry, a cyclic reaction exists in an enzymatic transformation of substrates into products in solution. If the activities of the substrate (S) and the product (P) in solution (where the reaction S → P is assumed to be negligibly slow) are maintained at suitable constant values far out of equilibrium with each other, the free energy difference of the substrate and the product will drive the reaction in a cyclic way as E → ES → EP → E. We refer this as a linear cycling steady state. Due to chemical reactions, the number of each species (N_E, N_{ES}, N_{EP}) in solution will fluctuate no matter whether the system is at equilibrium or at a cycling steady state. A general formalism for the calculation of the noise power density spectrum $G(\omega)$ in the quantity $N = \Sigma a_i N_i$ is presented, where N_i refers to the number of species i in solution and a_i is a constant. In equilibrium case, the noise power spectrum is always of Debye type: $G(\omega)$ is constant in the low frequency region and is proportional to ω^{-2} in the high frequency region. In cycling steady state case $G(\omega)$ may have Lorentzian terms and may show "peaking" at a certain frequency. This distinction in $G(\omega)$ could be useful in differentiating biochemical models. Some possible applications in biological systems are also discussed.

TH-PM-F12 ISOLATION AND CHARACTERIZATION OF MONOAMINE OXIDASE FROM HYPERFUNCTIONING HUMAN THYROIDS. A.Udupa,* S.Srinivasan and K.N.Udupa,* Department of Biophysics and Department of Surgery, Institute of Medical Sciences, Banaras Hindu University, Varanasi, India. (Intr. by D.R. Sanadi).

Monoamine oxidase is a mitochondrial enzyme which acts on monoamines such as NE and 5-HT by oxidative deamination. The enzyme is thought to be involved in thyroid disorders. The MAO was isolated from hyperfunctioning human thyroids. Histochemistry and histology of the tissues were done. PAGE studies revealed a single band indicating homogeneity. The elution profile from a DEAE column eluted with 0.01 M phosphate buffer resulted in three peaks. The active fraction subsequently concentrated, when loaded again on a DEAE column, resulted in essentially two peaks. The active concentrated fractions from this, analysed by a Sephadex G-200 column resulted in three units of molecular weights 220,000, 23,000, and 4,000 of which the last one was found to be active. Preliminary studies on MAO from hypofunctioning and malignant human thyroids have also been made. With this it is possible to propose a tentative model for the enzyme from hyperfunctioning human thyroids with three subunits out of which one or more could probably be common among the enzyme from hyperfunctioning, hypofunctioning and malignant human thyroids.